CHAPTER 4

RESULTS AND DISCUSSION

4.1 Characterization of synthesis of silicon carbide nanowires (SiCNWs)

4.1.1 Synthesis of SiCNWs without vacuum pump - assisted system

1) Characterization by SEM and TEM

After the synthesis by different heating and purification, the grayish products were obtained. Fig. 4.1 shows high magnification SEM images of a small quantity of nanowires and diameter distribution of all samples, all nanowires were randomly oriented on the substrate. fig. 4.1a shows curly and straight features of nanowires were synthesized at 1,200°C. Besides, fig. 4.1c and 1e show smooth and straight morphologies of nanowires were synthesized at the reaction temperature of 1,300°C and 1,400°C. These nanowires were obtained generally show the distribution diameter of 10-70 nm, 20-80 nm and 20-90 nm from different reaction temperatures at 1,200°C to 1400°C, the average of 39.80 nm, 40.67 nm and 48.44 nm diameters, respectively. Moreover, fig. 4.1c clearly shows the spherical droplets of nickel particles acted as catalyst at the tip of each nanowires, it can be indicated that these nanowires were grown via the vapor–liquid–solid (VLS) growth mechanism.

From diameter distribution graphs, the diameters of nanowires were measured in the area of 3x4 μm. It can be seen that the nanowires from the highest reaction temperature have a larger and wider distribution diameter than others. All products almost have a length of about micron.

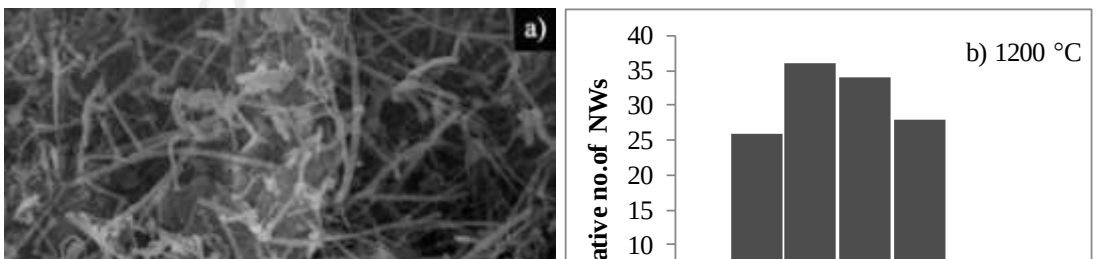

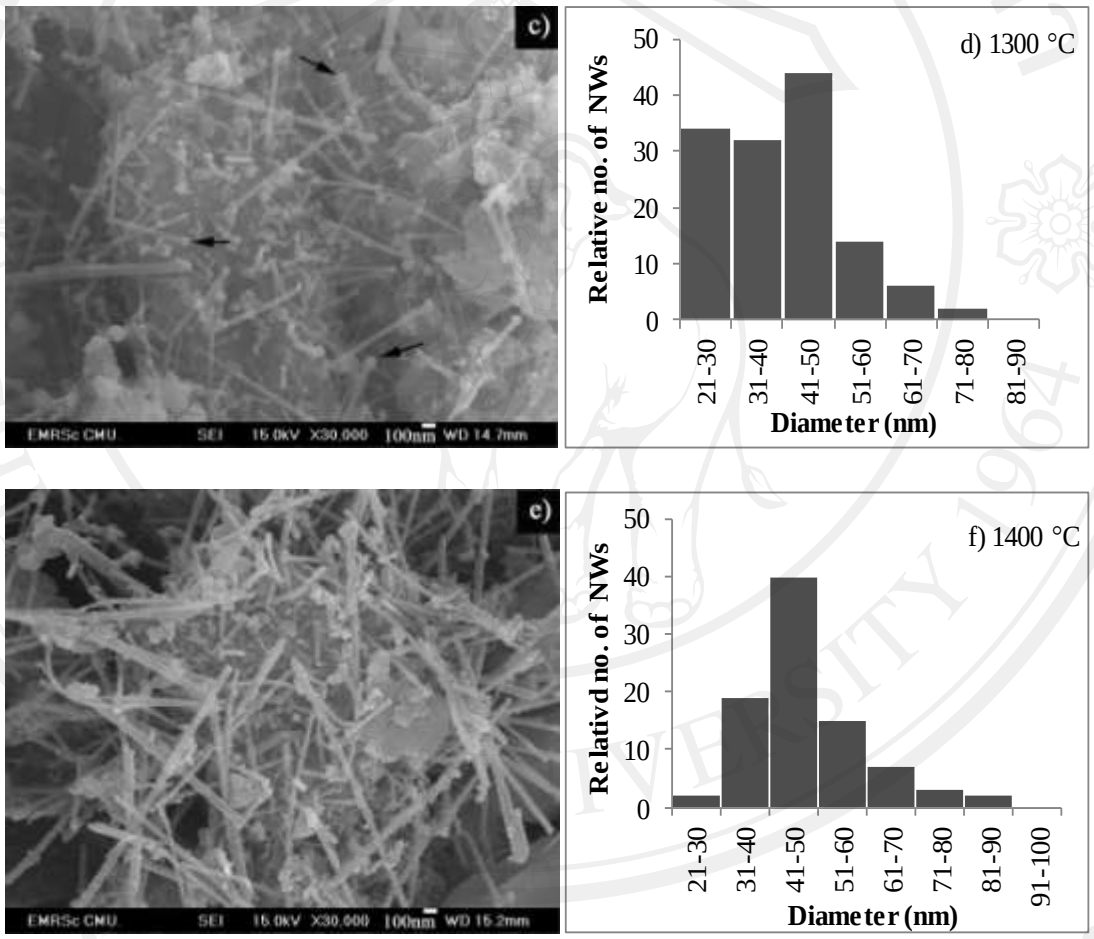

Figure 4.1 FE-SEM images of as-products by different reaction temperatures and the diameters distribution of nanowires (a), (b) at 1,200°C, (c), (d) at 1,300 °C, and (e), (f) at 1,400 °C

For more details, TEM was taken to investigate further structure of all products. The nanowire were obtained from reaction temperature at 1,200°C is shown

in fig. 4.2a which indicates an amorphous structure. fig. 4.2b shows the nanowire was synthesized at 1,400°C which the structure to be similar in the case of reacted temperature at 1,300°C. Besides, the SAED pattern (inset) shows more details about the nanowire, and the clear spots indicated that the nanowire is a single crystal and the zone axis is consequently determined to be [011]. Moreover, it can be seen that the metal catalyst droplet on the tip of nanowire which confirmed that the nanowires from this experiment were fabricated via VLS growth mechanism.

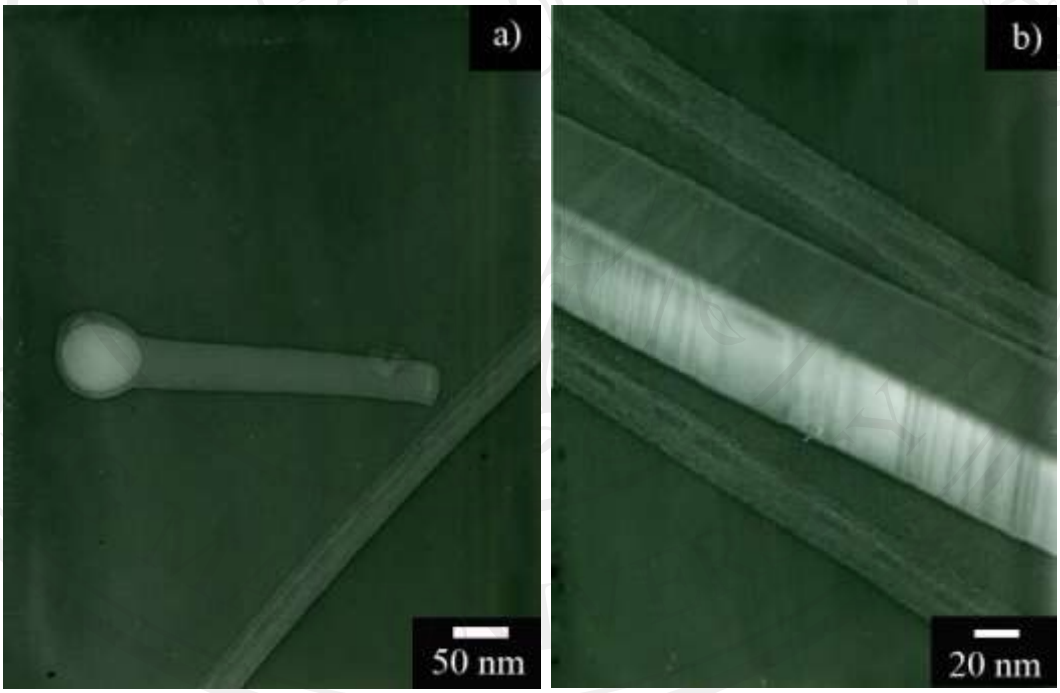

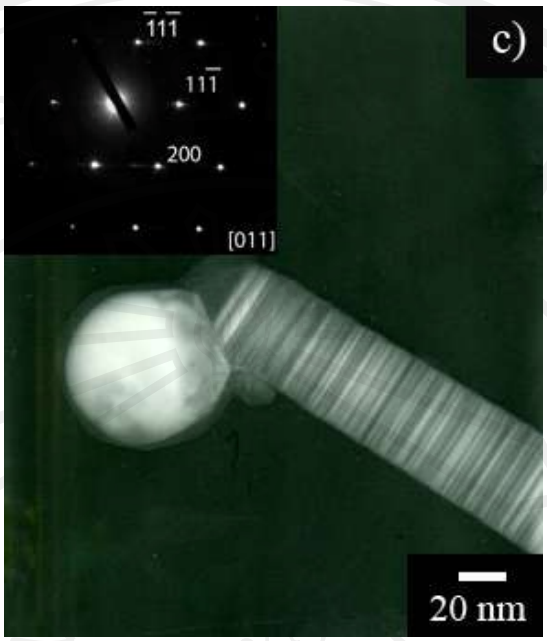

Figure 4.2 Typical TEM images of SiCNWs formed with different temperatures; a) 1,200°C, b) 1,300°C and c) 1,400°C

2) X-Ray Diffraction Results

The XRD pattern of nanowires were obtained from different synthesis temperatures is shown in fig. 4.3. There are five peaks in the spectrum agreeing well with the known values of (111), (200), (220), (311) and (222) diffraction peaks of cubic β-SiC. Corresponding to the Si powder was also found. Especially at lowest reaction temperature (1,200°C) shows the stronger peak than other. Besides, strong and weak peaks of C were found at 1,200°C and 1,300°C reaction, respectively. It can be seen that there is an amount of carbon and silicon acted as sources remain in the system. On the other hand, growth reactions of nanowires are incomplete formation at 1,200°C and almost complete at 1,300°C.

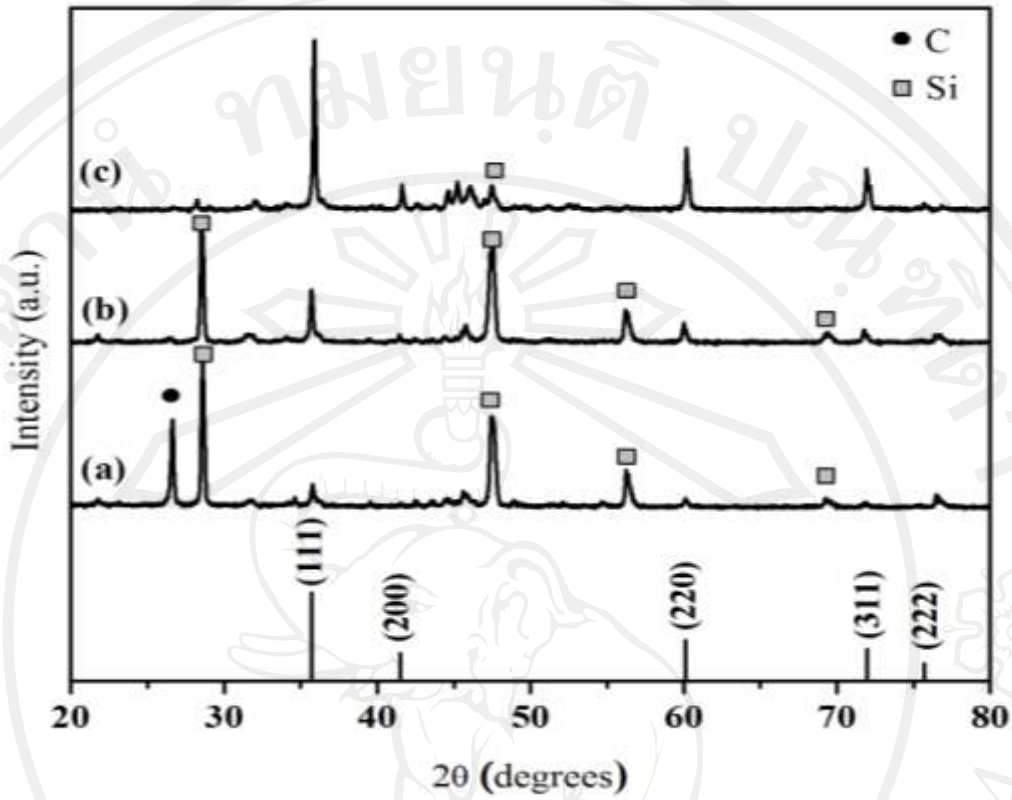

Figure 4.3 X-ray diffraction spectra of products from different reaction temperatures at: a) 1,200°C, b) 1,300°C and c) 1,400°C. It can be indexed to be β-SiC (JCPDS Card No. 73-1665)

4.2.1 Synthesis of SiCNWs with vacuum pump - assisted system

4.2.1.1 Using Fe_2O_3 as Catalyst

1) Characterization by SEM and TEM

After the synthesis by CVD method and heat-treated at 700°C for 4 h, the as-obtained of product possess remaining of 60% by weight with white-wool like features were formed on as-grown powder surfaces that is SiO_2 nanofibers whereas, the dark gray powders become to the light green-gray products as shown in fig. 4.4.

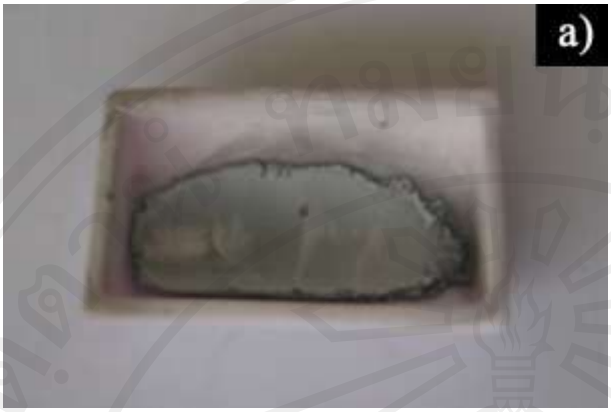

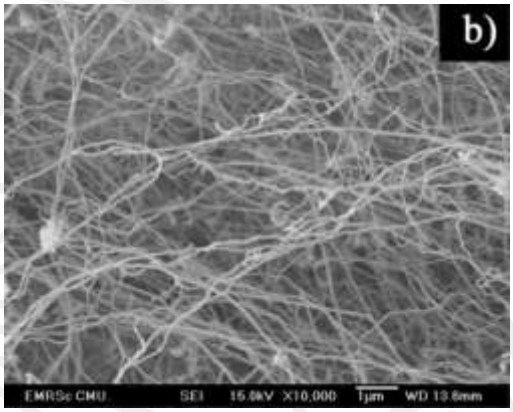

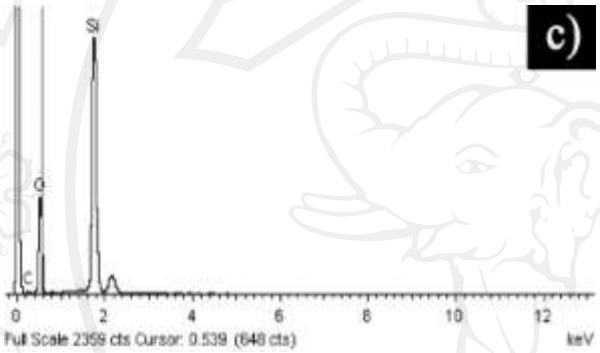

Element	Weight%	Atomic%
C K	3.78	6.24
O K	48.41	60.00
Si K	47.81	33.75
Totals	100.00	

Figure 4.4 a) Photograph of the product in alumina boat from Fe_2O_3 catalyst b) FE-SEM image of white wool-like from a), and c) shows the corresponding EDS spectra.

The white wool–like products are thought to be SiO_2 that confirmed with EDS spectra is given by fig. 4.4c. The EDS mass ratio reveals that these nanofibers consisted of Si, O and C. The mass ratio of Si to O (Si:O) is 1:1.01 and the atomic ratio is 1:1.78 and this composition is very close to stoichiometric SiO_2 composition.

Fig. 4.5 shows SEM images of all samples, the nanowires were randomly oriented with almost curly structure. The nanowires collected from reaction temperature at 1300°C show shorter wires than other with the length of about a micron, while the nanowires from reaction temperature at 1350°C and 1400°C reveal the length up to several micrometers.

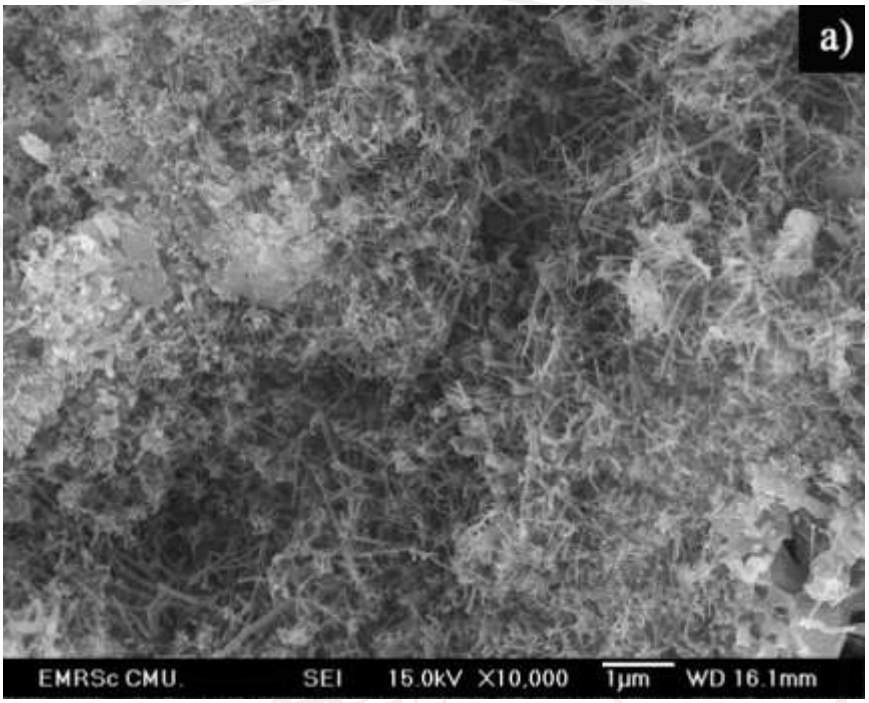

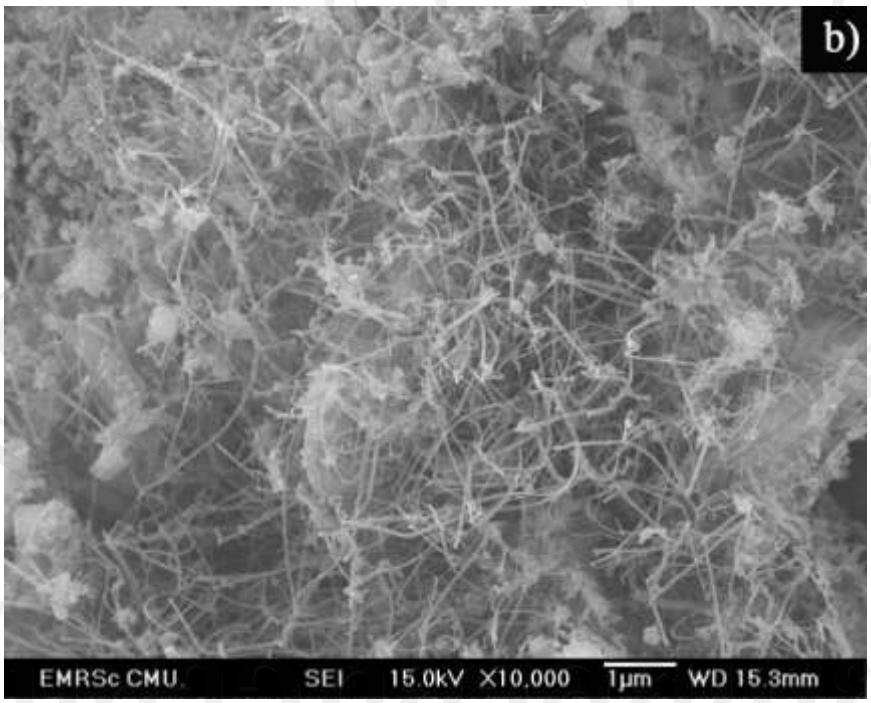

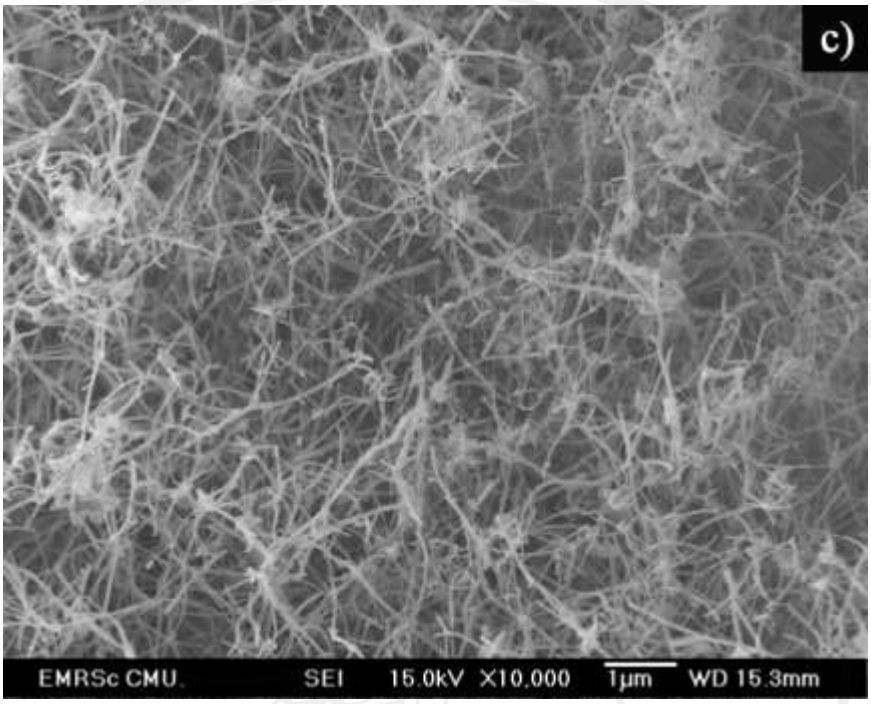

Figure 4.5 FE-SEM images of using Fe_2O_3 as catalyst with the reaction temperature at: a) 1,300°C, b) 1,350°C and c) 1,400°C

Fig. 4.6 shows the SiCNWs were fabricated from using Fe_2O_3 as catalyst with different reaction temperature at 1,300°C -1,400°C and their diameter distribution.

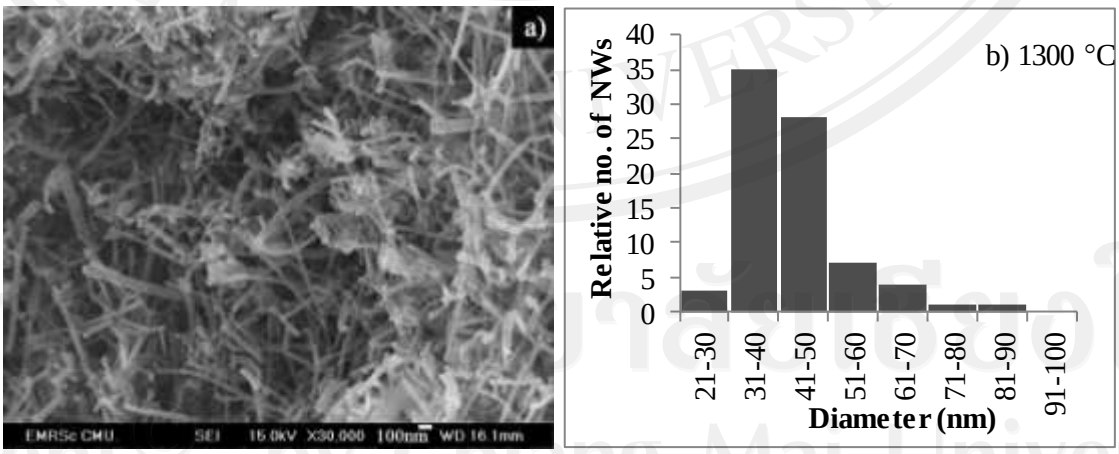

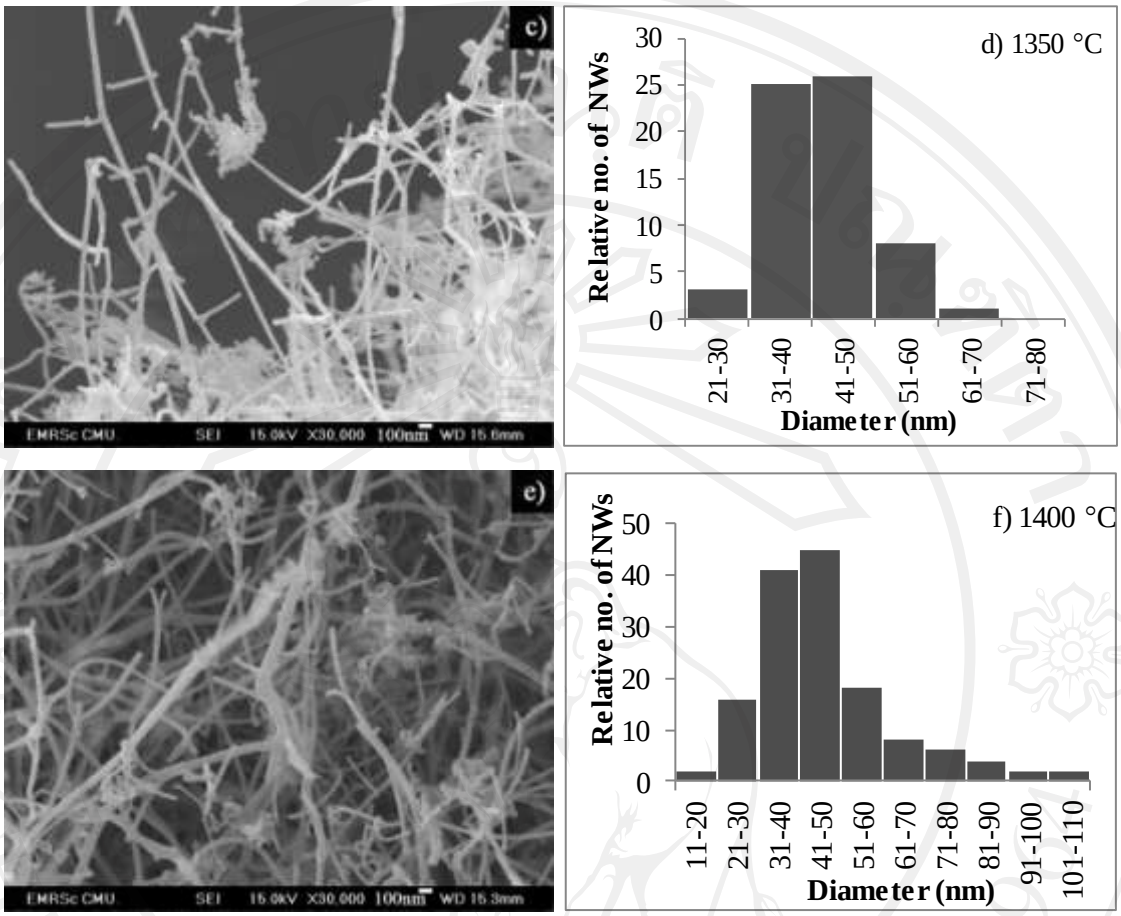

Figure 4.6 Distributions of nanowires diameters using Fe_2O_3 as catalyst with different temperature; a) 1,300°C, b) 1,350°C and c) 1,400°C

Distributions of nanowires diameters were obtained from three differences temperature. These nanowires were started to be counted and arranged from the smallest to the largest values. The nanowires were reacted of 1,300°C, 1,350°C and 1,400°C very well distributed with the average of 42.65 nm and 41.29 nm and 47.26 nm diameters, respectively. The results of measurement in the case of synthesis at 1,300°C and 1,350°C show the mostly ranges of 31-50 nm in diameters, while the nanowires at 1,400°C shows widest ranges distributed diameter.

In order to characterize the structure in further details, the products were investigated by TEM and selected area electron diffraction (SAED). The white wool-like products covered the surface were peeled off, some of pale green-gray products were dispersed in ethanol, and dropped on the copper grid covered with carbon film. Fig. 4.7a shows the nanowires were obtained from using Fe_2O_3 as catalyst with reaction temperature at 1,300°C, 1,350°C and 1,400°C, which the diameter about 20.50 nm, 20.45 nm and 19.64 nm, respectively. Electron diffraction was done to determine its structure (in the inset of fig. 4.7a, which the clearly spots suggested that the nanowire is a single crystal and the zone axis is consequently determined to be [011]. However, it cannot be found stacking faults that are perpendicular to the wire axis. All nanowires were obtained from different temperature reveal formation of crystalline was not very well. It may be possible that there are a few amounts of Fe liquid droplets due to Fe_2O_3 compound decomposed at 1,566°C [97], which higher than reaction temperatures, it may be affected to SiC nuclei growth to the nanowires. Besides, ball of them were wrapped with thin SiO_2 layer.

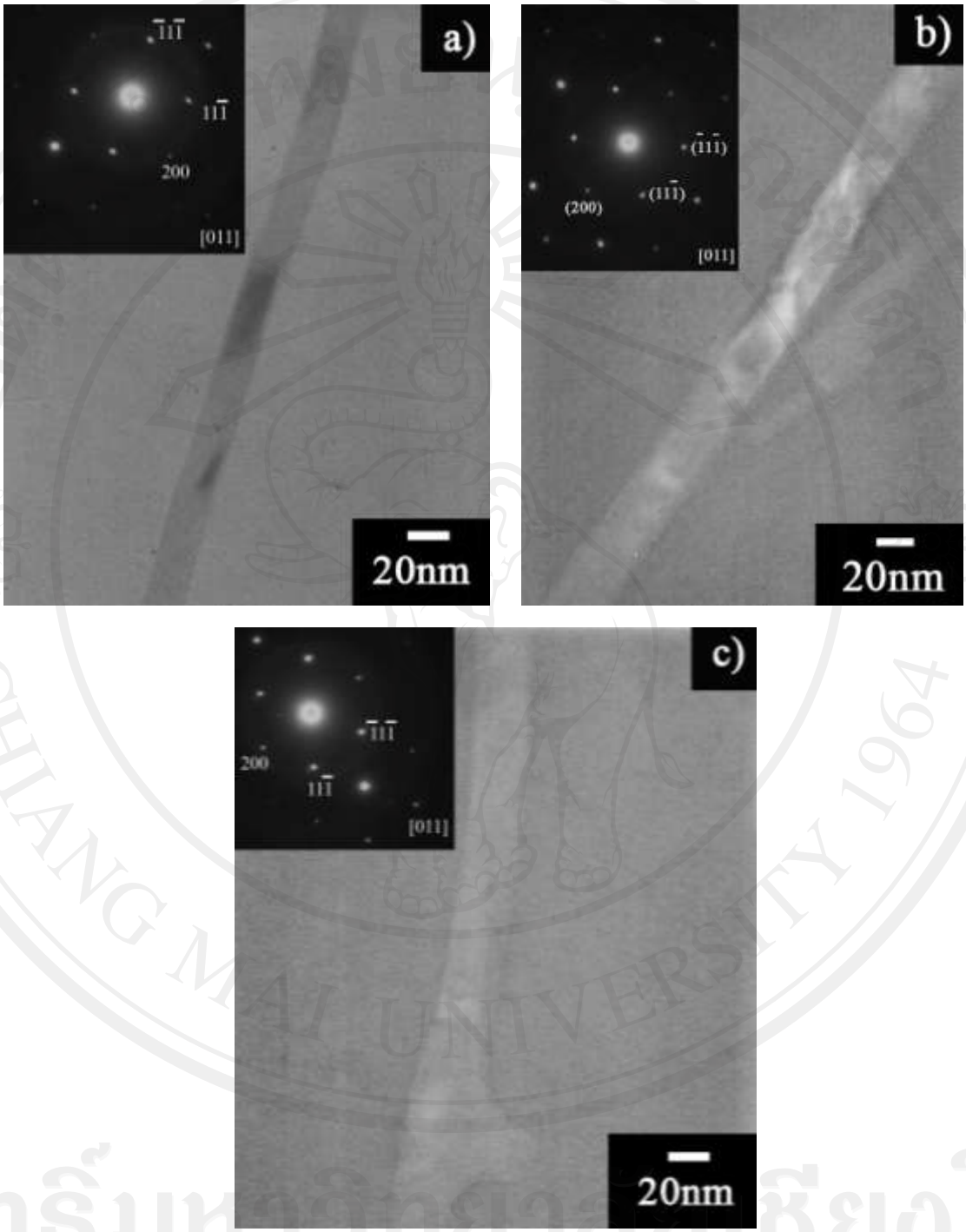

Figure 4.7 Typical TEM images of SiCNWs were obtained from using Fe_2O_3 as catalyst and its SEAD patterns from varying temperatures at a) 1,300°C, b) 1,350°C, and c) 1,400°C

2) X-Ray Diffraction Results

The XRD pattern of these nanowires is shown in fig. 4.8. There are five peaks in the spectrum agreeing well with the known values of (111), (200), (220), (311) and (222) diffraction peaks of cubic β-SiC. Diffraction peaks of reaction at 1300°C are weaker than other and all products have a weak diffraction peak of Ni and C elements which decreased corresponds to increasing of reaction temperature. This result exhibits that an amount of carbon and Si acted as sources remaining in the system, which confirmed incomplete nanowires growth. In additional, a weak diffraction peak of FeSi at 45.4° has been detected. The eutectic point of Fe and Si is about 1207°C, which indicated that FeSi phase was formed during the growth process [93, 98].

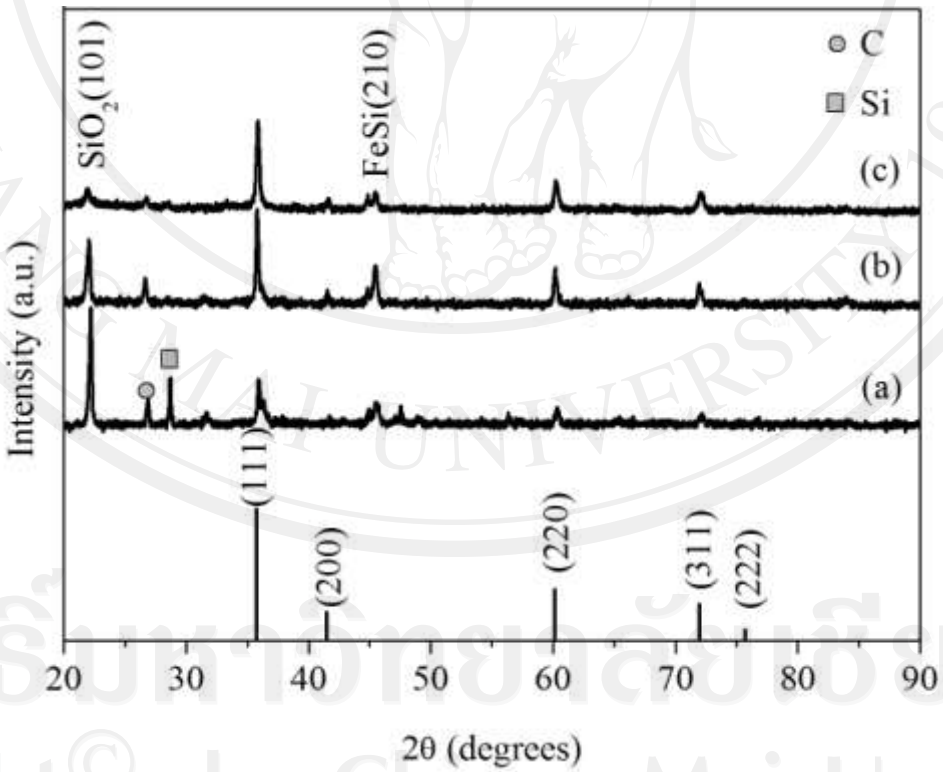

Figure 4.8 X-ray diffraction spectra of products: using Fe2O3 as catalyst after heat-treated a) 1,300°C, 1,350°C and 1,400°C. It can be indexed to be β-SiC (JCPDS Card No. 73-1665)

Fig. 4.9 reveals the high resolution TEM images, it can be seen that the SiC nanowire possess a high density of stacking faults which are perpendicular to the wire axis. The crystal lattice image clearly shows that the spacing of lattice fringes is 0.25 nm as shown in fig. 4.9 which is corresponds to the {111} planes spacing of cubic SiC. It further demonstrates that the angle of lattice fringes between [111] and the wire axis is 73° which is very close to the angle between of $(\bar{1}1\bar{1})$ plane and $(11\bar{1})$ plane (70.53°) of 3C–SiC, suggest that the nanowire grew along [111] direction. From these results, the growth direction of all nanowires can be assumed to be [111] direction.

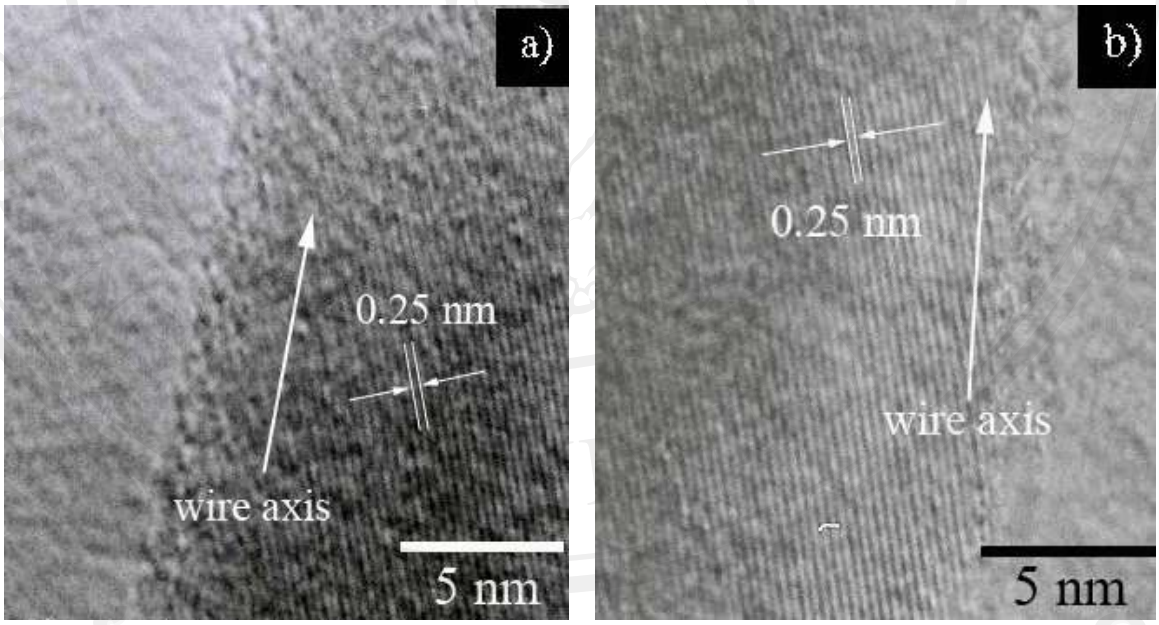

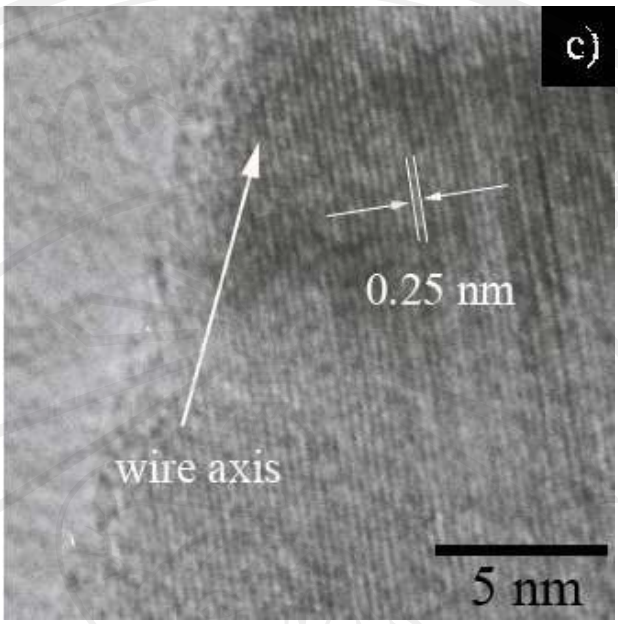

Figure 4.9 HR-TEM images of SiCNWs synthesized by using Fe_2O_3 as catalyst with varying temperatures at a) 1,300°C, b) 1,350°C and c) 1,400°C

4.2.1.2 Using Ni_2O_3 as Catalyst

In order to obtain the optimum condition, SiCNWs have been synthesized by varying temperature of 1,300°C, 1,350°C and 1,400°C.

1) Characterization by SEM and TEM

After the synthesis by CVD method and purification, the as-obtained product possesses remaining of 60% by weight. All of samples, the gray powders became light green-gray powders with white wool-like covers the surfaces were shown in fig. 4.4a. Fig. 4.10 shows the typical structures of the synthesized nanowires by SEM images. The as-obtained of all products have white wool-like features were formed on the surfaces as shown in fig. 4.10a that is SiO_2 nanofibers are similar to that of fig. 4.4b. A large quantity of SiCNWs with straight wire-like structures is shown in fig. 4.10b. EDS spectra of these nanowires have been synthesized at 1,350 °C is given in

fig. 4.10c which indicated that these of nanowires were composed of Si, C, O and Ni elements. The atomic ratio of Si:C is 42.12:41.75 and this composition is very close to stoichiometric SiC. The weak Ni peak came from the catalyst. Also synthesis of nanowires at temperature of 1,300 °C and 1,400°C were obtained with the same results.

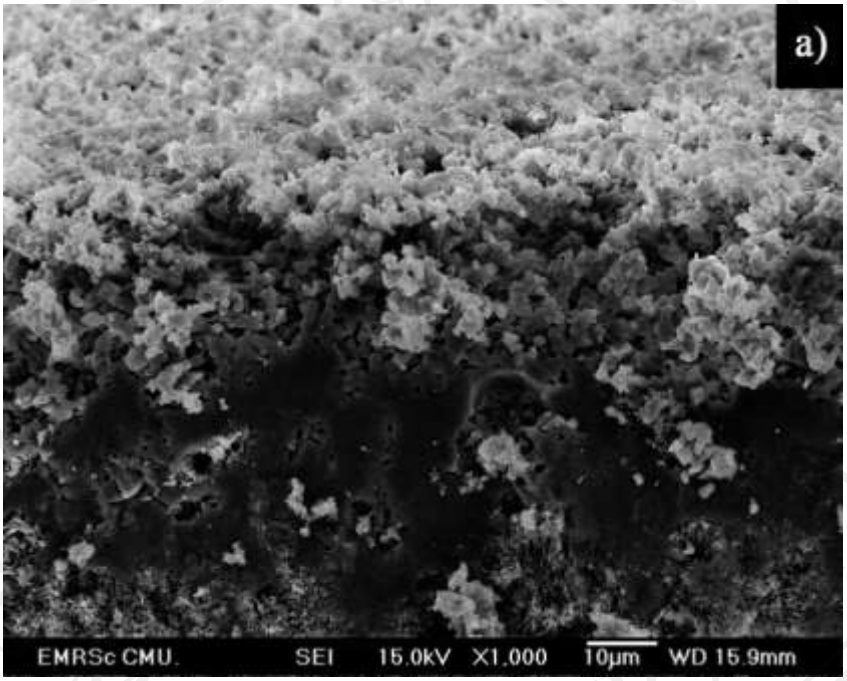

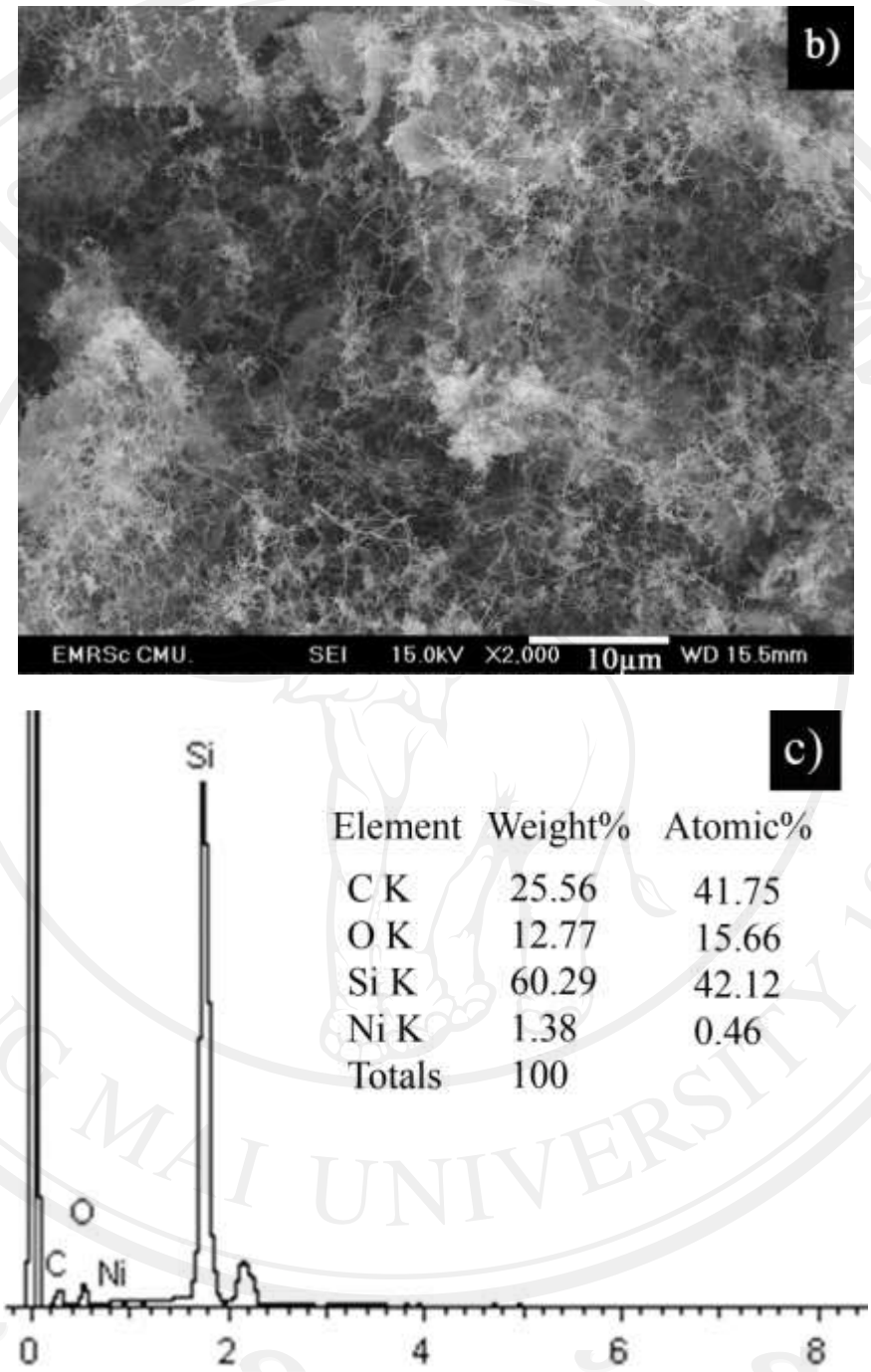

Figure 4.10 SEM images of a) the cross section of white wool-like features covered as-grown powder, b) FE-SEM image of surface of the white wool-like product at 1,350°C, and c) is the corresponding EDS spectra.

To investigate their morphologies and distribution diameters of all products, the typical structures of these nanowires were observed by magnified SEM images as shown in fig. 4.11. It can be seen that all nanowires have a smooth and clearly surfaces with randomly arrays and both straight and curly wires lengths up to several micrometers.

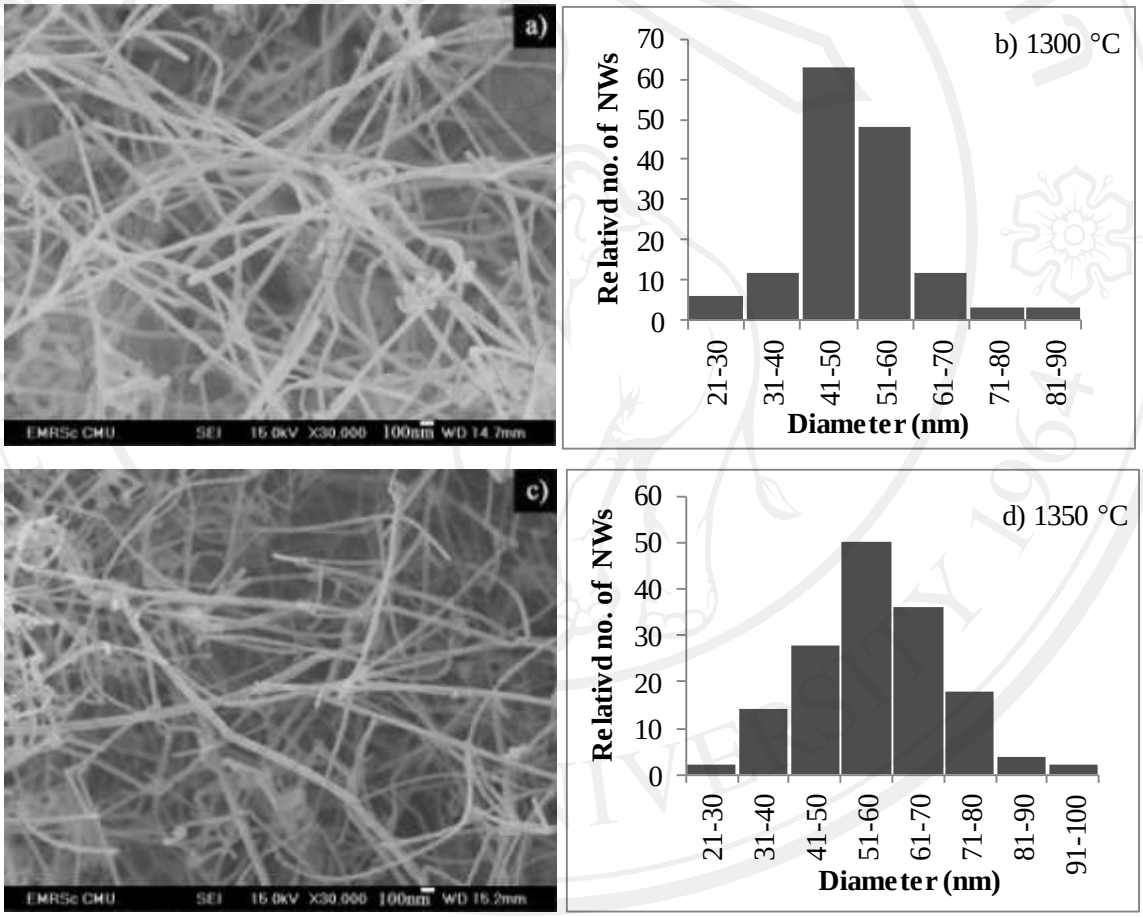

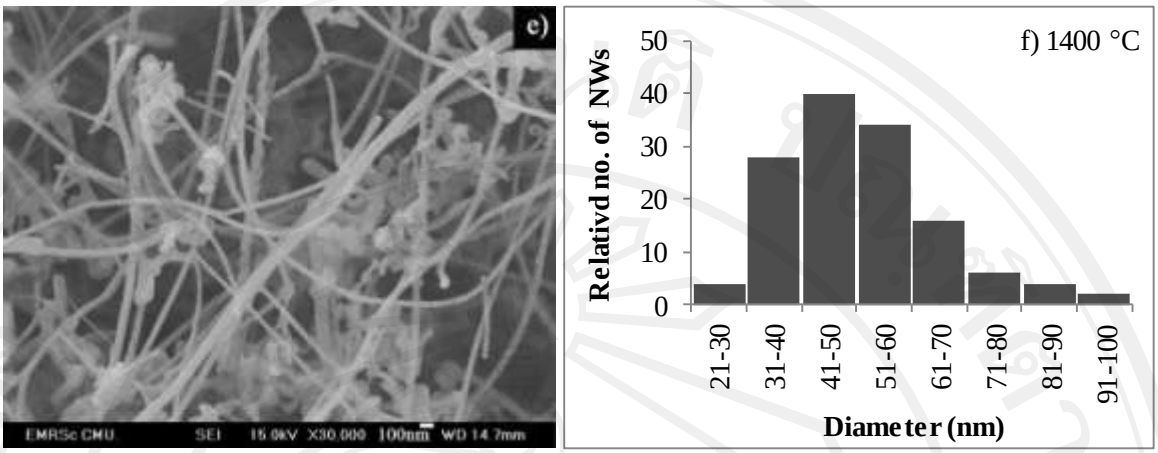

Figure 4.11 FE-SEM images of as-products by different temperatures and the distribution of nanowires diameters (a), (b) at 1,300°C, (c), (d) at 1,350 °C and (e), (f) at 1,400 °C

Distributions of nanowires diameters were obtained from three differences temperature. These nanowires were started to be counted and arranged from the smallest to the largest values. The nanowires were reacted of 1,350°C and 1,400°C very well distributed with the average of 54.64 nm and 51.31 nm diameters, respectively. The result of measurement in the case of synthesis at 1,300°C shows the mostly ranges of 41-60 nm in diameters with the average of 48.88 nm.

In order to characterize the structure in further details, the as-grown products were investigated by TEM and the SAED patterns as shown in fig. 4.12. The nanowires were characterized with SiC crystalline core and amorphous SiO_2 shell structure. SAED patterns (inset) show clear spots indicated that the core of nanowire is a single crystalline structure. Comparison of all nanowires which were synthesized by different temperatures, it can be seen that the nanowires were taken from the different reaction temperatures of 1,300°C, 1,350°C and 1,400°C have the diameter of

core of about 37 nm, 31 nm and 37 nm and it was wrapped with a uniform layer of shell with a thickness of about 22 nm, 14 nm and 3 nm, respectively. It can be seen that the nanowire was obtained from the lowest reaction temperature has the thickest layer of amorphous and significantly decrease of the layer according to increasing of reaction temperature. The SAED pattern in fig. 4.12a (inset) shows clear spots indicated that the nanowire is a single crystal. The diffraction pattern can be indexed to 3C-SiC, which grown along the [111] direction.

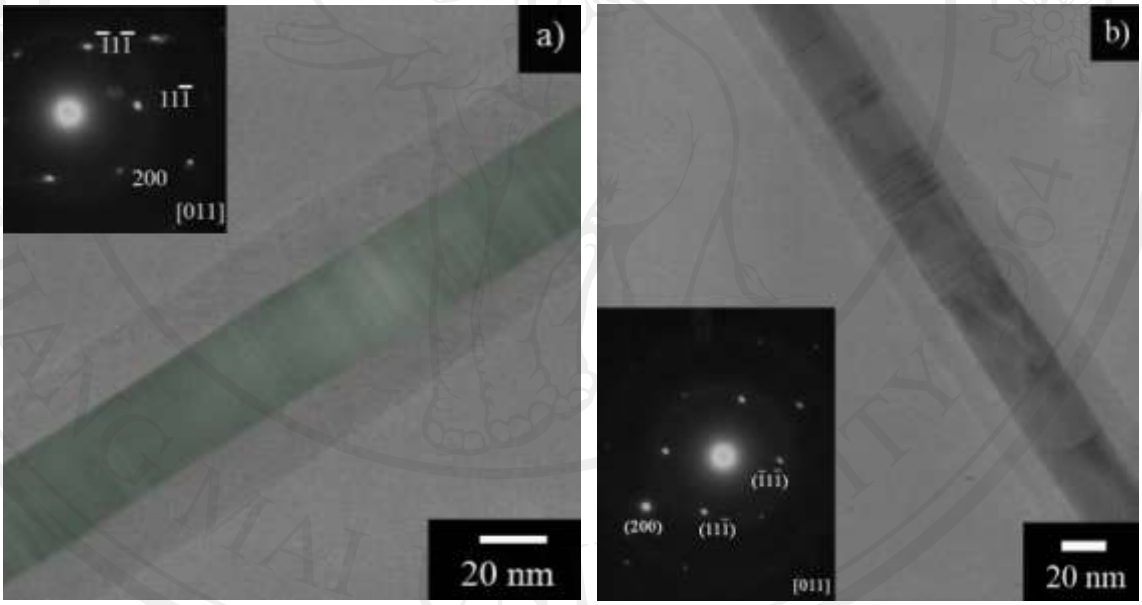

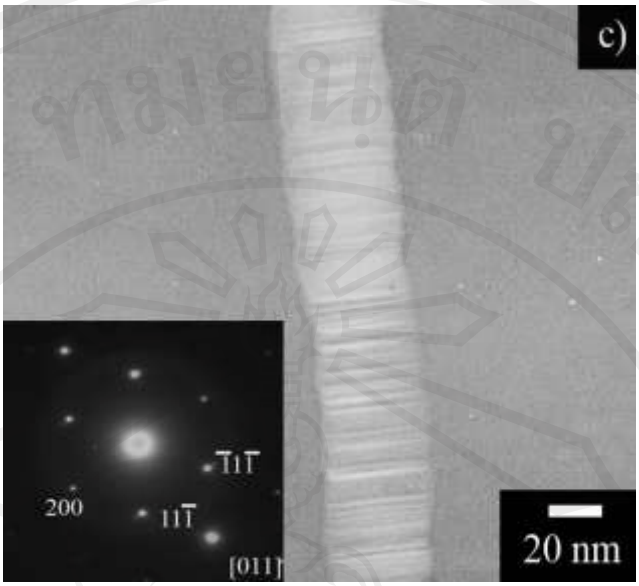

Figure 4.12 Typical TEM images of SiCNWs and its SEAD patterns from varying temperatures at a) 1,300°C, b) 1,350°C and c) 1,400°C

Fig. 4.13 reveals the high resolution TEM images, it can be seen that the SiC nanowire possess a high density of stacking faults which are perpendicular to the wire axis. The crystal lattice image clearly shows that the spacing of lattice fringes is 0.25 nm as shown in fig.4.13c which is corresponds to the {111} planes spacing of cubic SiC. It further demonstrates that the angle of lattice fringes between [111] and the wire axis is 73° which is very close to the angle between of $(\bar{1}1\bar{1})$ plane and $(11\bar{1})$ plane (70.53°) of 3C–SiC, suggest that the nanowire grew along [111] direction. From these results, the growth direction of the nanowires can be assumed to be [111] direction.

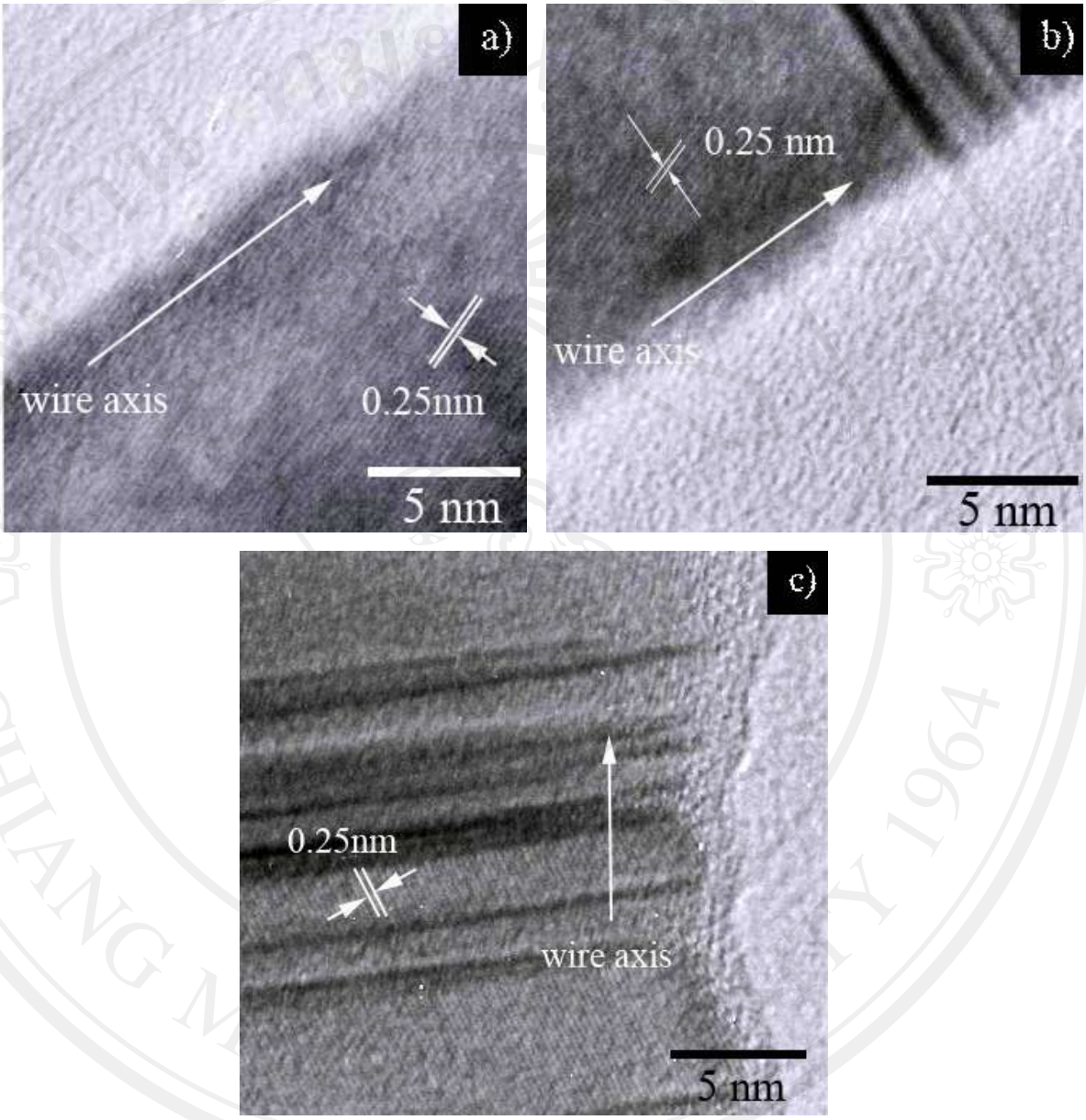

Figure 4.13 HR-TEM images of SiCNWs synthesized by varying temperatures at a) 1,300°C, b) 1,350°C and c) 1,400°C

2) X-Ray Diffraction Results

Phase identifications of the products were characterized by XRD as show in fig. 4.14. There are five peaks in the spectrum agreeing well with the known values of (111), (200), (220), (311) and (222) diffraction peaks of cubic β-SiC (JCPDS card no.

73-1665) as shown in fig 4.14 corresponding to SEM and TEM results. There is a small peak of Si in reaction temperature at 1,300°C, while reaction temperature at 1,350°C shows slightly stronger peaks than other.

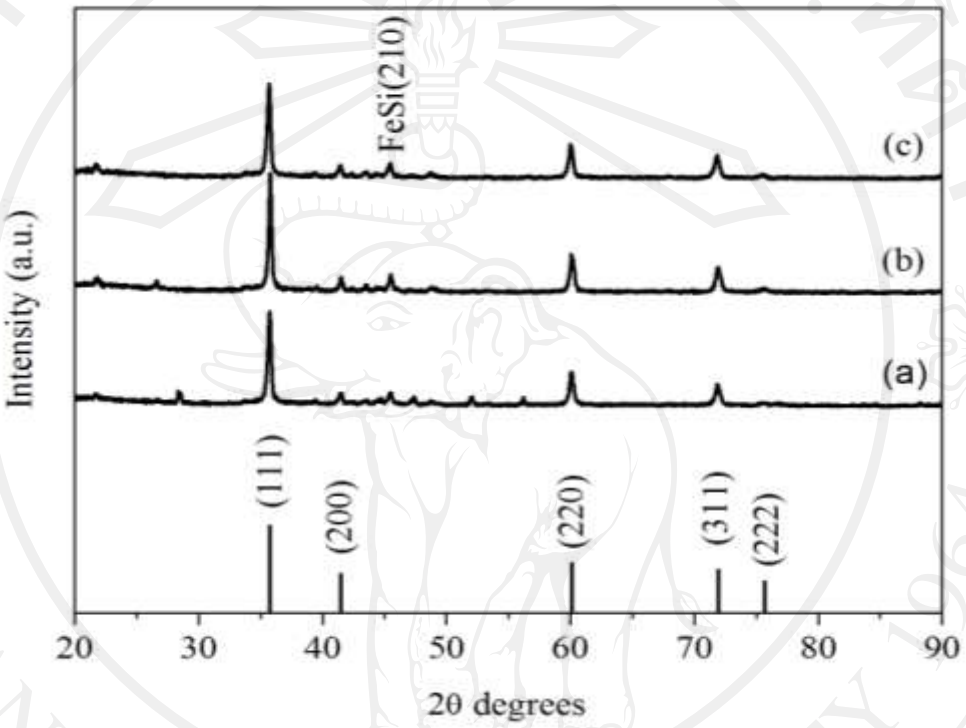

Figure 4.14 X-ray diffraction spectra of products: after heat-treated a) 1,300°C, 1,350°C and 1,400°C. It can be indexed to be β-SiC (JCPDS Card No. 73-1665)

3) FTIR Results

Fig. 4.15 shows the FT-IR spectrum of the nanowires, which has two absorption bands from Si-O stretching vibration at about and 1093 and 474 cm^{-1} transversal optic (TO) mode of Si-C vibration at about 804 cm^{-1}. The results indicated that the nanowires were composed of SiC and amorphous SiO_2 and corresponding with previous reports [99].

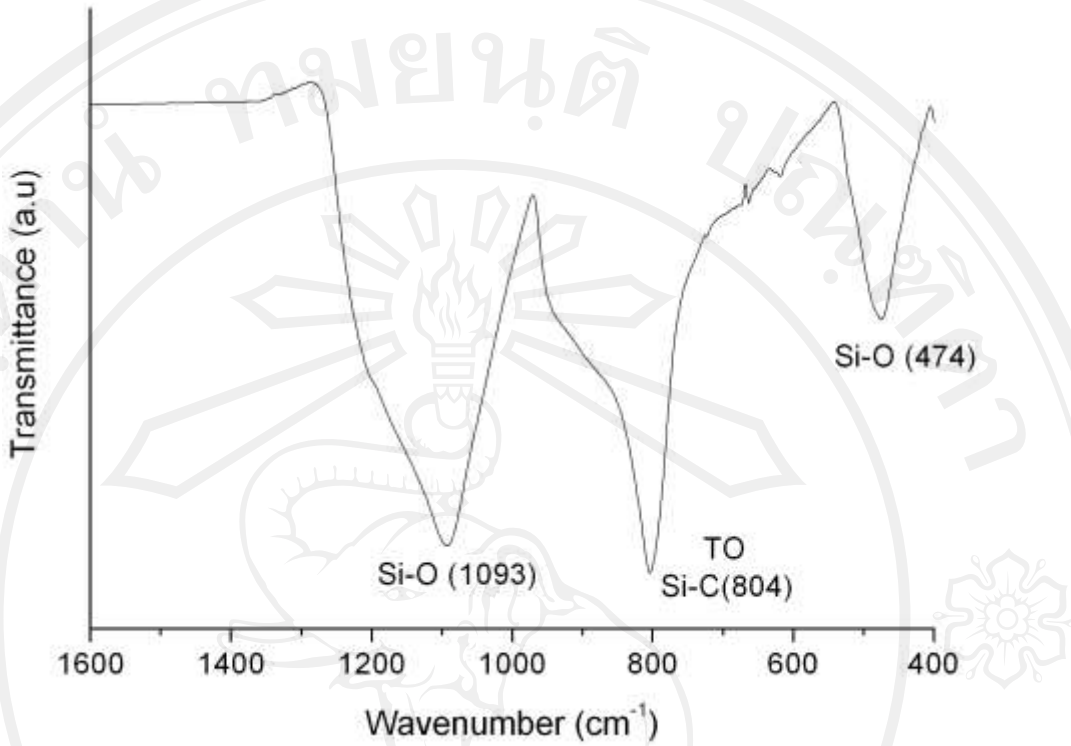

Figure 4.15 FT-IR spectrum of SiCNWs products synthesized at 1,350°C

4.2.3 Growth mechanism

The vapor-liquid-solid mechanism for the growth of SiC whiskers initiated by a metal catalyst has been suggested by Wanger and Ellis [93] and Urretavizcaya and Lopez [100]. In this experiment, Ni_2O_3 are employed as catalyst to fabricate SiC nanowires. Moreover, TEM also show the existence of metal catalyst at the tip of SiCNWs as shown in fig. 4.2c. This fact suggested that Ni_2O_3 catalyst play a key role in the formation of SiC nanowires and a VLS mechanism in the most probable growth mechanism. The growth process in these experiments was formed through these three reactions as follows. Firstly, as the temperature increased to the reaction temperature then, the SiO vapors are generated by reaction (4.1) between Si and residual O_2 in the system during heat

$$2Si\ (s) + O_2\ (v) \rightarrow 2SiO(v) \qquad (4.1)$$

Alloying initiates at above 900 °C, at this stage Ni exists in mostly solid state and CO vapor is also generated (4.2 and 4.3)

$$2C\ (s) + O_2\ (v) \rightarrow 2CO(v) \qquad (4.2)$$

$$3C(s) + Ni_2O_3(s) \rightarrow 2Ni(s) + 3CO(v) \qquad (4.3)$$

With increasing amount of SiO and CO vapor condensation and dissolution, Si, C and Ni form an alloy and liquefy. The volume of the alloy droplet increases, the process of nucleation of the nanowire begins (4.4).

$$SiO(v) + CO(v) \rightarrow SiC\ (s) + SiO_2\ (s) \qquad (4.4)$$

Once the SiC nanocrystal nucleates at the liquid/solid interface, further condensation/dissolution of the vapor into the system increases the amount of SiC precipitation from the alloy. The interface is then pushed forward (or backward) to form nanowires [20, 94, 101, 102]. The growing progress of nanowires ends until the vapor sources are exhausted or the catalyst loses activity.

4.2 Fabrication of CNTs, SiCNWs and Epoxy Resin Nanocomposites

The nanocomposites were prepared with different ratios of 0.5-8 vol% of CNTs and SiCNWs fillers which were mixed in the epoxy resin matrix and tested tensile strength as shown in fig. 4.16.

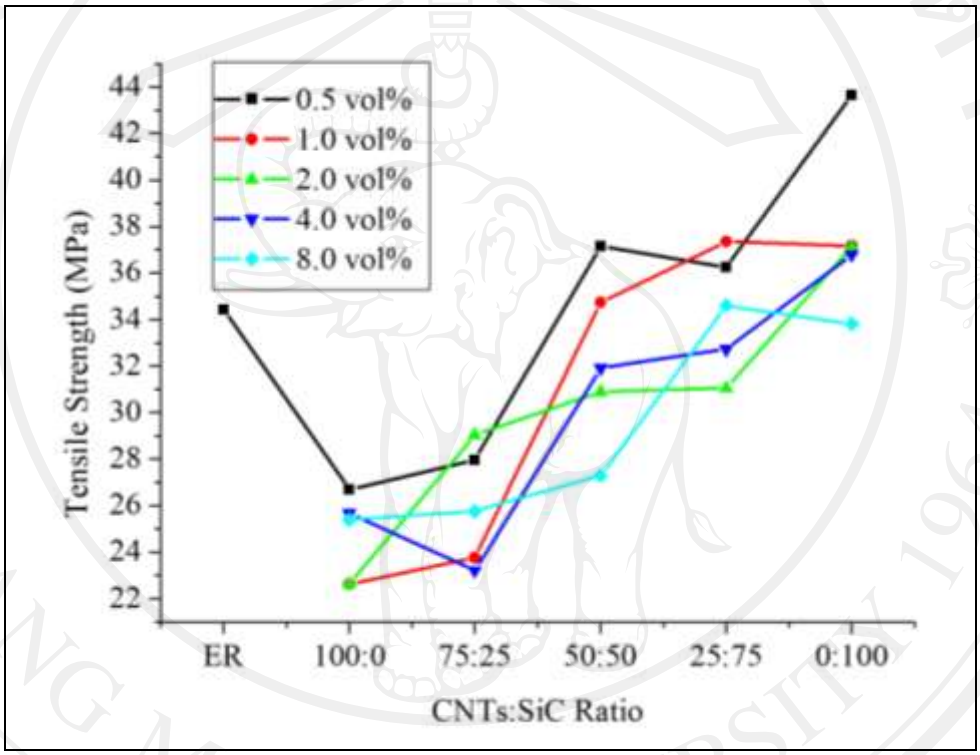

Figure 4.16 Tensile strength of epoxy resin matrix and CNTs, SiCNWs fillers with different ratios of 0.5-8.0 vol%

From fig. 4.16, the result exhibits that strength simultaneously decrease according to increasing the fillers. Especially, adding more contents of CNTs affect to decreasing of the strength. However, adding only SiCNWs in the matrix shows the highest strength. In order to get the best results, author decided to repeat the

fabrication of the nanocomposites by decrease contents of the fillers with different ratios of 0.05-0.2 vol%.

4.2.1 The morphologies of CNTs and SiCNWs

Field emission scanning electric microscopy (FESEM) of the random CNTs and SiCNWs are shown in fig. 4.17a and b, respectively. As can be seen from fig. 4.17a, CNTs with diameters in ranges of 50-100 nm were highly entangled and randomly organized. The microstructures of SiCNWs are illustrated in fig. 4.17b. shows with diameters in ranges of 40-110 nm. The density of CNTs and SiCNWs were taken as 2.0 g cm^{-3}[24] and 0.996 g cm^{-3}[103], respectively. Moreover, before and after morphologies of the samples for tensile, compressive and impact tests as shown in fig.4.18 - 4.20, respectively.

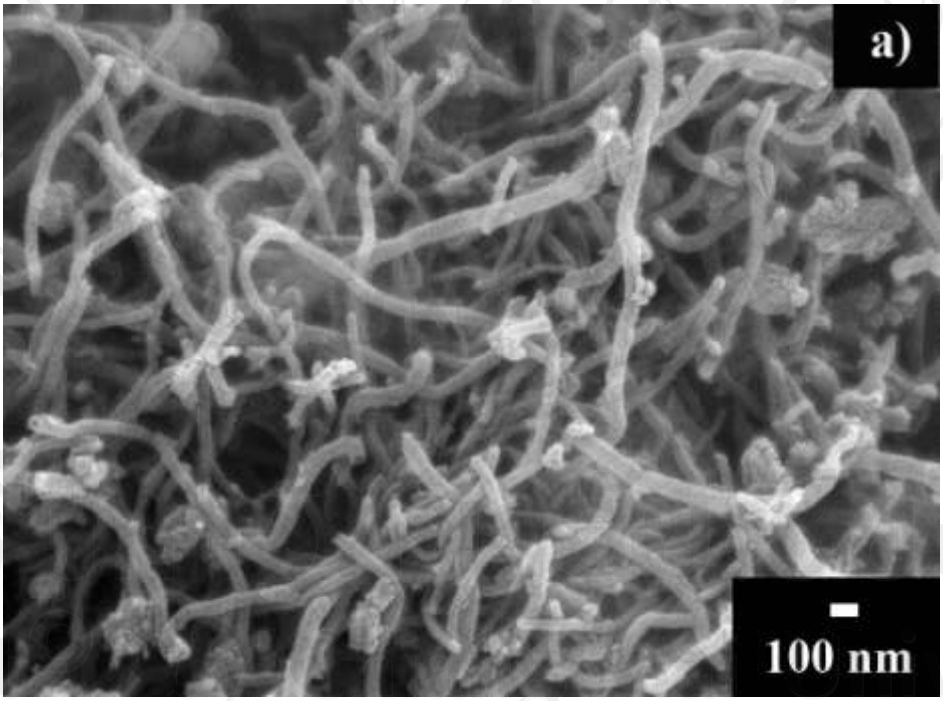

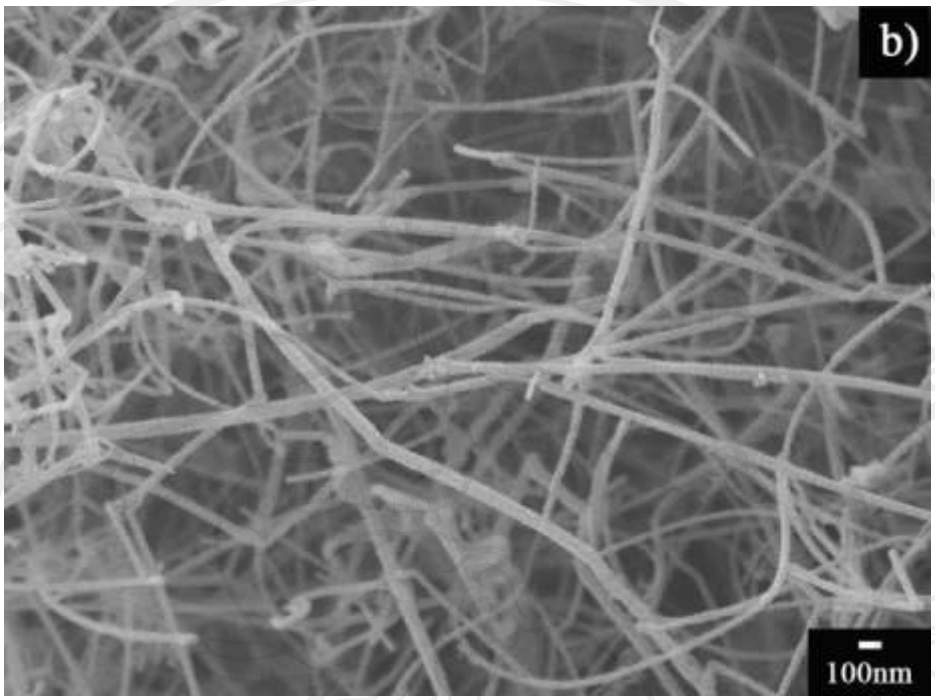

Figure 4.17 FE-SEM images of: a) CNTs and b) SiCNWs

4.2.2 The morphologies of nanocomposites samples

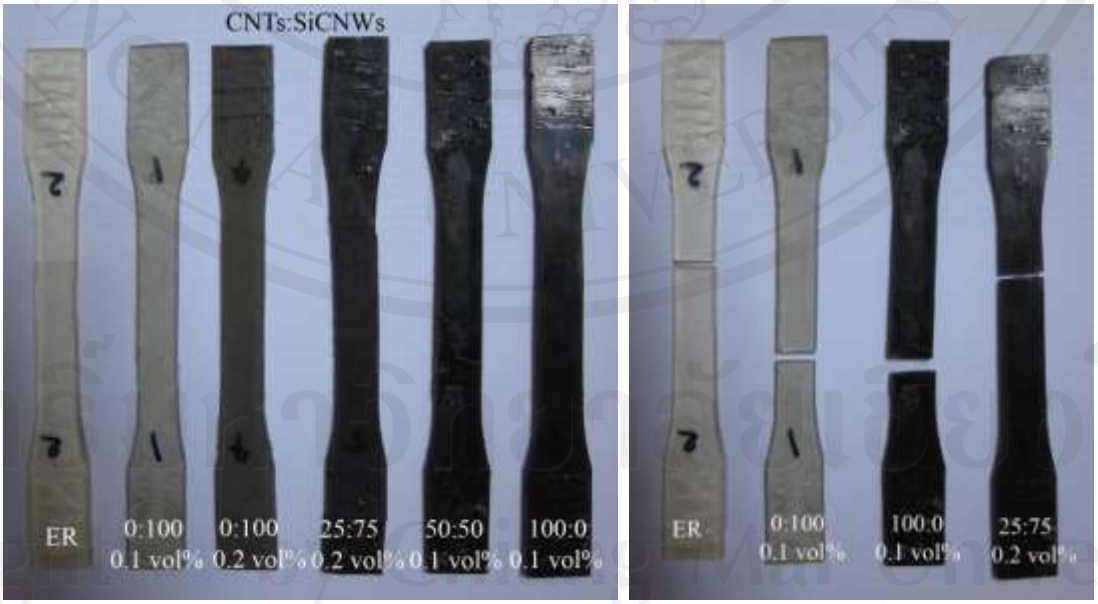

Figure 4.18 Before and after tensile test of CNTs, SiCNWs and epoxy matrix samples

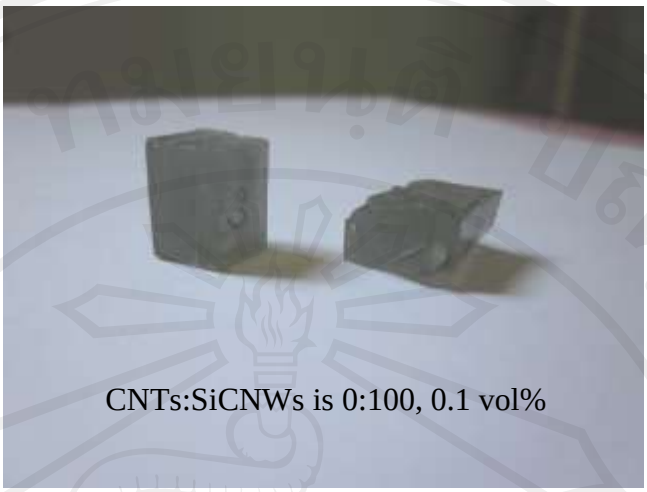

Figure 4.19 Before and after compressive test of CNTs, SiCNWs and epoxy matrix samples

Figure 4.20 Before (CNTs:SiC ratio and after impact test of CNTs, SiCNWs and epoxy matrix samples

4.2.3 Effect of fillers on the mechanical properties of epoxy composites

Table 1 shows the density of epoxy resin nanocomposites were reinforced with CNTs and SiCNWs. The results show the density of nanocomposites samples that increased consistent with increasing of the fillers content, which is clearly more than neat epoxy resin (1.1586 g cm^{-3}). Besides, the nanocomposites were varied the

ratio of CNTs:SiCNWs of each volume percent, the density slightly increased as the SiCNWs content increased.

Table 4.1 The density data for CNTs, SiCNWs and epoxy resin nanocomposites

Ratio of CNTs:SiCNWs	**Content of the fillers (vol %)**		
	0.05	**0.10**	**0.20**
Epoxy	1.1586		
100:0	1.1605	1.1616	1.1626
75:25	1.1604	1.1622	1.1631
50:50	1.1598	1.1629	1.1642
25:75	1.1603	1.1625	1.1643
0:100	1.1626	1.1653	1.1696

*The unit of density = g cm^{-3}

Tensile and compressive responses of nanocomposites are shown in fig. 4.21 and 4.22, it is can be seen that epoxy with nano-fillers have the higher strength than neat epoxy and increased simultaneously with the addition of CNTs and SiCNWs which indicated that the addition of these nano-fillers could promote the strength of the composites. Moreover, the results exhibited that the ratio of CNTs:SiCNWs is 25:75 at 0.2 vol%, the tensile and compressive strength have the maximum values of 48.59 MPa and 122.30 MPa, respectively.

Fig. 4.23 shows absorbed energy of samples were tested by Charpy impact test which indicated that the absorbed energy increased corresponds to increasing of content of the fillers. Moreover, the results also exhibited that the ratio of CNTs:SiCNWs is 25:75 at 0.2 vol%, the absorbed energy has the maximum value of 0.28 J correspond to the results of tensile and compressive tests.

The samples were added either SiCNWs or CNTs, it were found that both nano-fillers added samples show similar strength. Except in the case of 0.2 vol%, the SiCNWs added samples shows clearly higher strength than CNTs added samples. Possible reasons for such behavior could be that there are more impurities contents in CNTs powder and agglomeration of CNTs than SiCNWs powder, due to treatment by acid-treated with 1 vol% of mixed acids could not remove all impurities and can be seen clearly when added more contents of CNTs powder in the matrix.

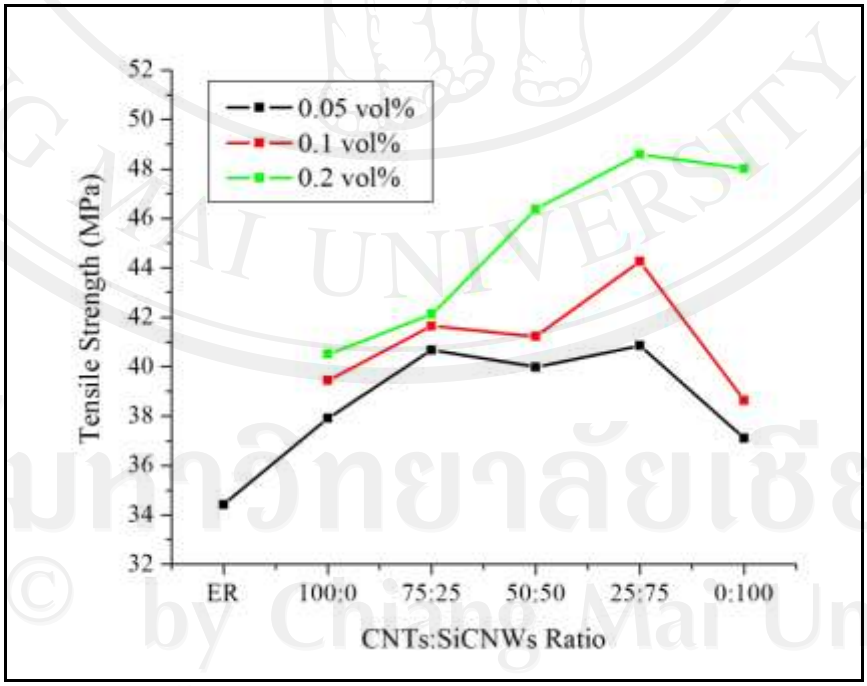

Figure 4.21 The tensile response of CNTs and SiCNWs loading content (vol %) on epoxy nanocomposites

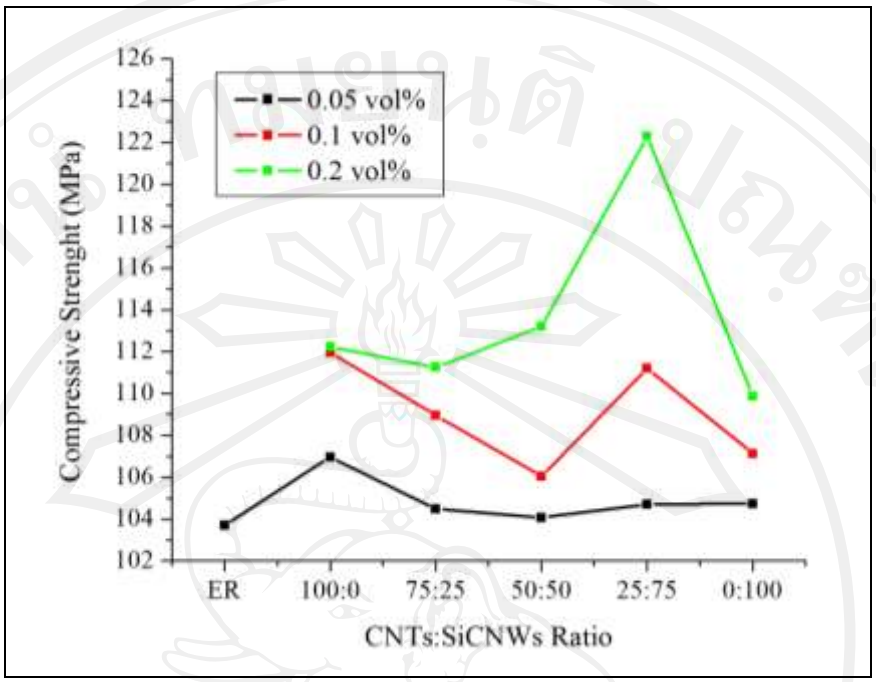

Figure 4.22 The compressive strength of CNTs and SiCNWs loading content (vol %) on epoxy nanocomposites

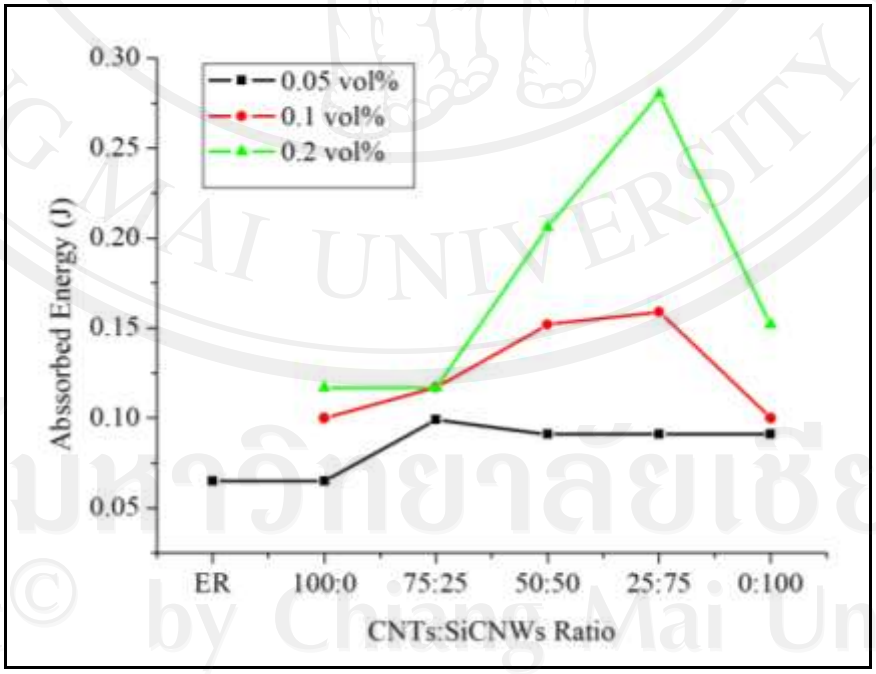

Figure 4.23 The impact strength of CNTs and SiCNWs loading content (vol %) on epoxy nanocomposites

Gain tensile, compressive and impact strength of the ratio of 25:75 (CNTs:SiCNWs; 0.2 vol%) is about 41.13%, 17.65 %, 332.64% respectively over the neat epoxy as shown in fig. 4.24- 4.26. Adding SiCNWs content was 75 parts mixed with 25 parts of CNTs content on condition 0.2% volume provided the highest gain in percentage of tensile test. However, there are no significantly gains of compressive test in the same condition.

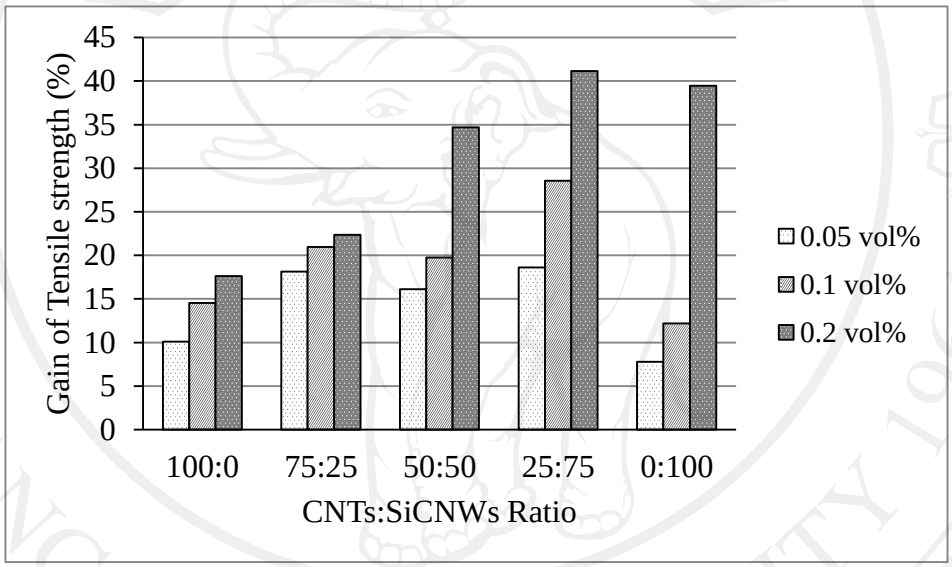

Figure 4.24 Gain tensile strength in percentage of nanocomposites with different ratios of CNTs, SiCNWs fillers

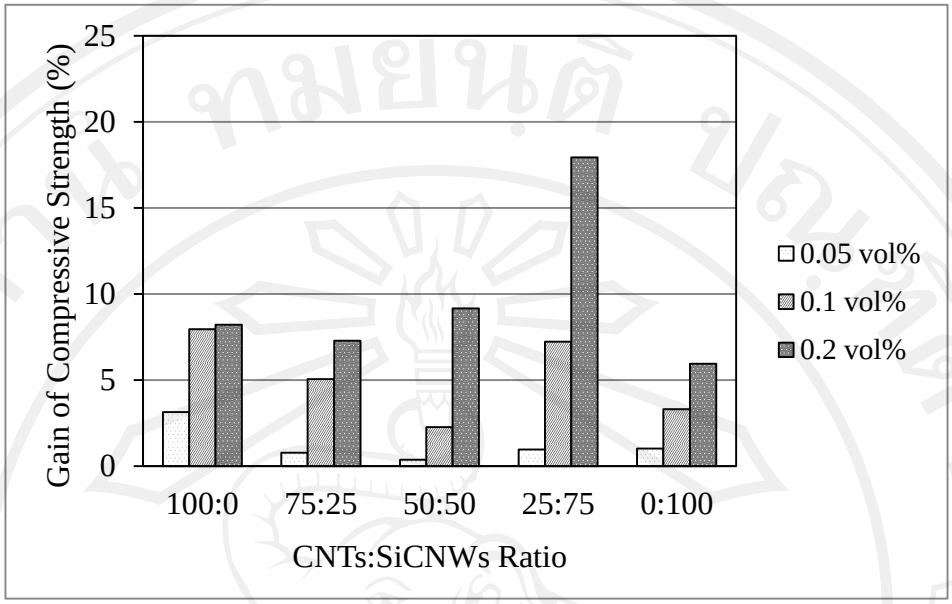

Figure 4.25 Gain compressive strength in percentage of nanocomposites with different ratios of CNTs, SiCNWs fillers

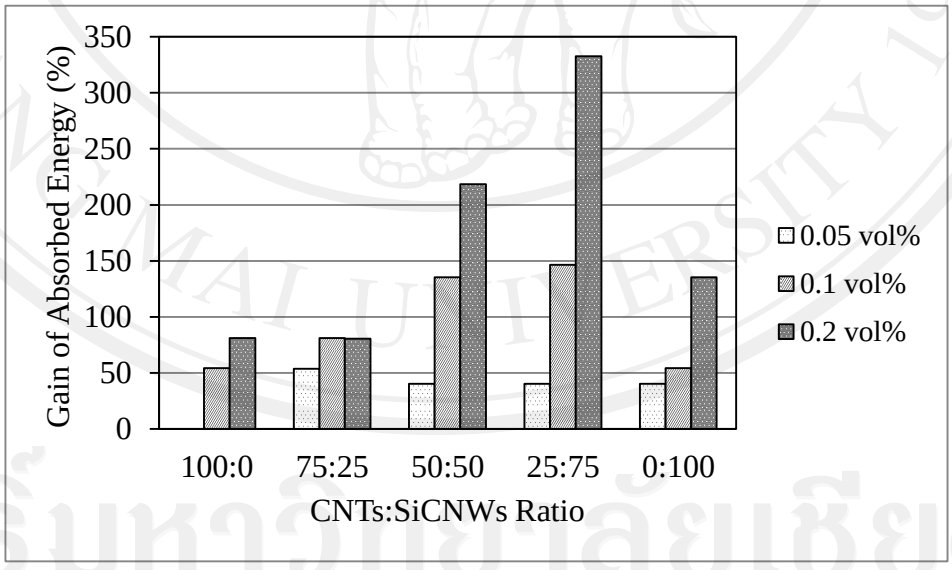

Figure 4.26 Gain of absorbed energy in percentage of nanocomposites with different ratios of CNTs, SiCNWs fillers

Furthermore, it is observed that the wear track values are shown in fig. 4.27 which reveals the range of 253.88 – 497.70 μm, while fig. 4.28 shows the wear rate of the nanocomposites samples with the range of 0.29 -2.19 μm^2. It exhibits that the wear rate are dramatically decreased with increasing of the fillers contents as compared to the neat epoxy resin. . Adding SiCNWs content was 75 parts mixed with 25 parts of CNTs content on condition 0.2% volume provided the highest wear resistance which possible reason might be slide friction properties of CNTs improve the resistance in the matrix. It might be concluded that the wear resistance of the nanocomposites samples could be improved by using the CNTs and SiCNWs fillers. The loss of wear track (48.99%) and wear rate (86.89%) as shown in fig. 4.29 and fig. 4.30 confirmed improvements of these fillers on the resin epoxy. Besides, fig. 4.31 – 4.33 show the photographs of the width of wear track of composites samples.

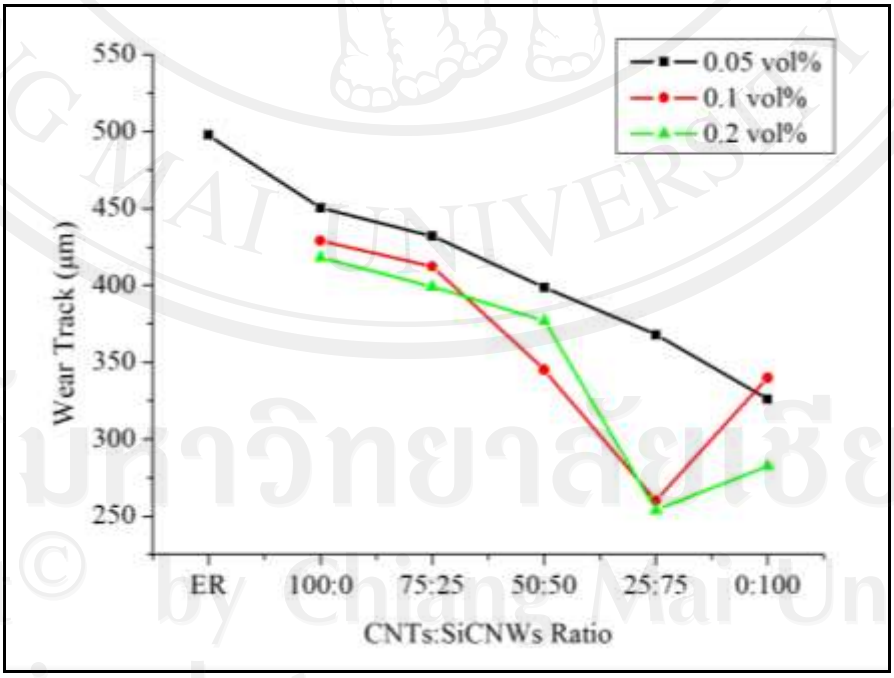

Figure 4.27 The wear track of nanocomposites samples with different ratios of the fillers

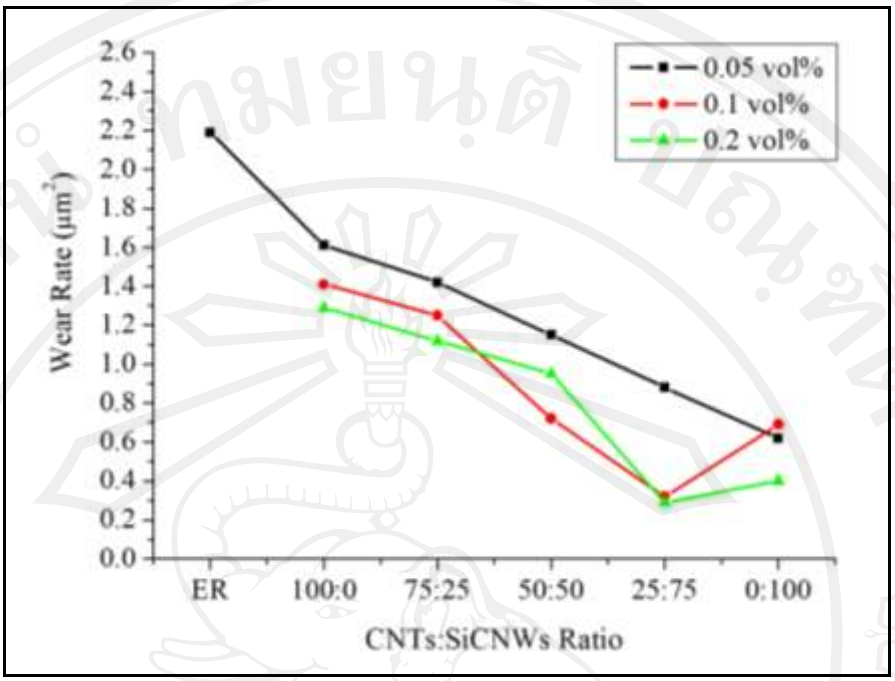

Figure 4.28 The wear rate of CNTs and SiCNWs loading content (vol %) on epoxy nanocomposites

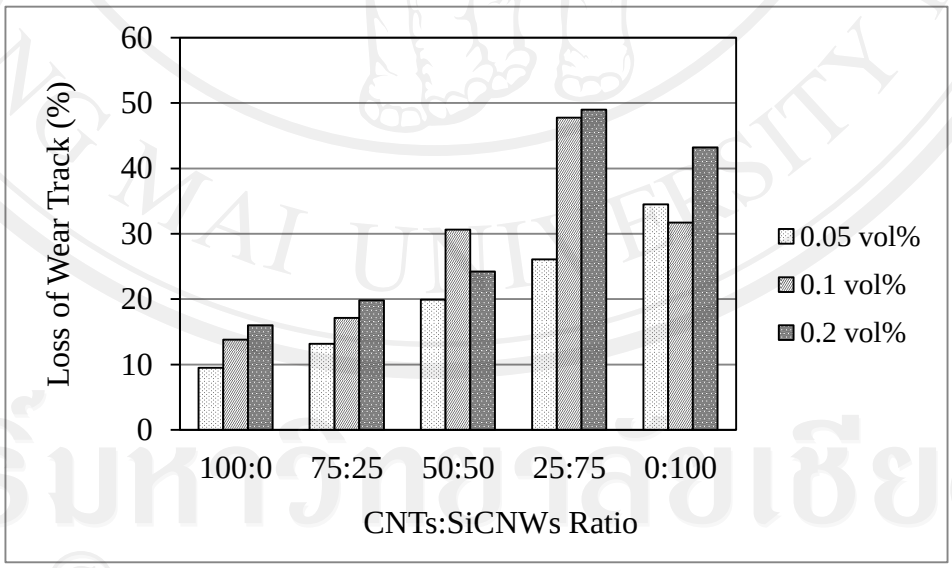

Figure 4.29 Loss of wear track in percentage of nanocomposites with different ratios of CNTs, SiCNWs fillers

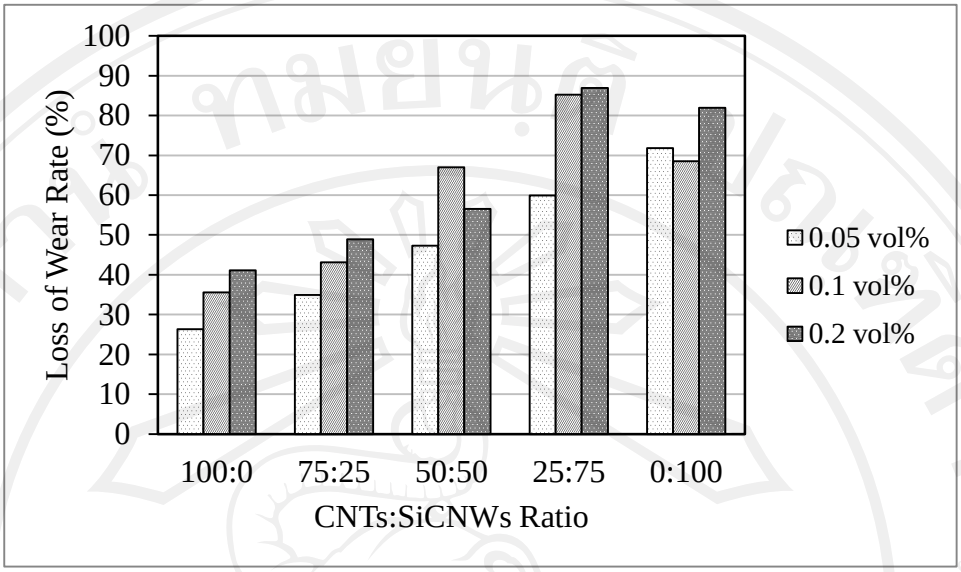

Figure 4.30 Loss of wear track in percentage of nanocomposites with different ratios of CNTs, SiCNWs fillers

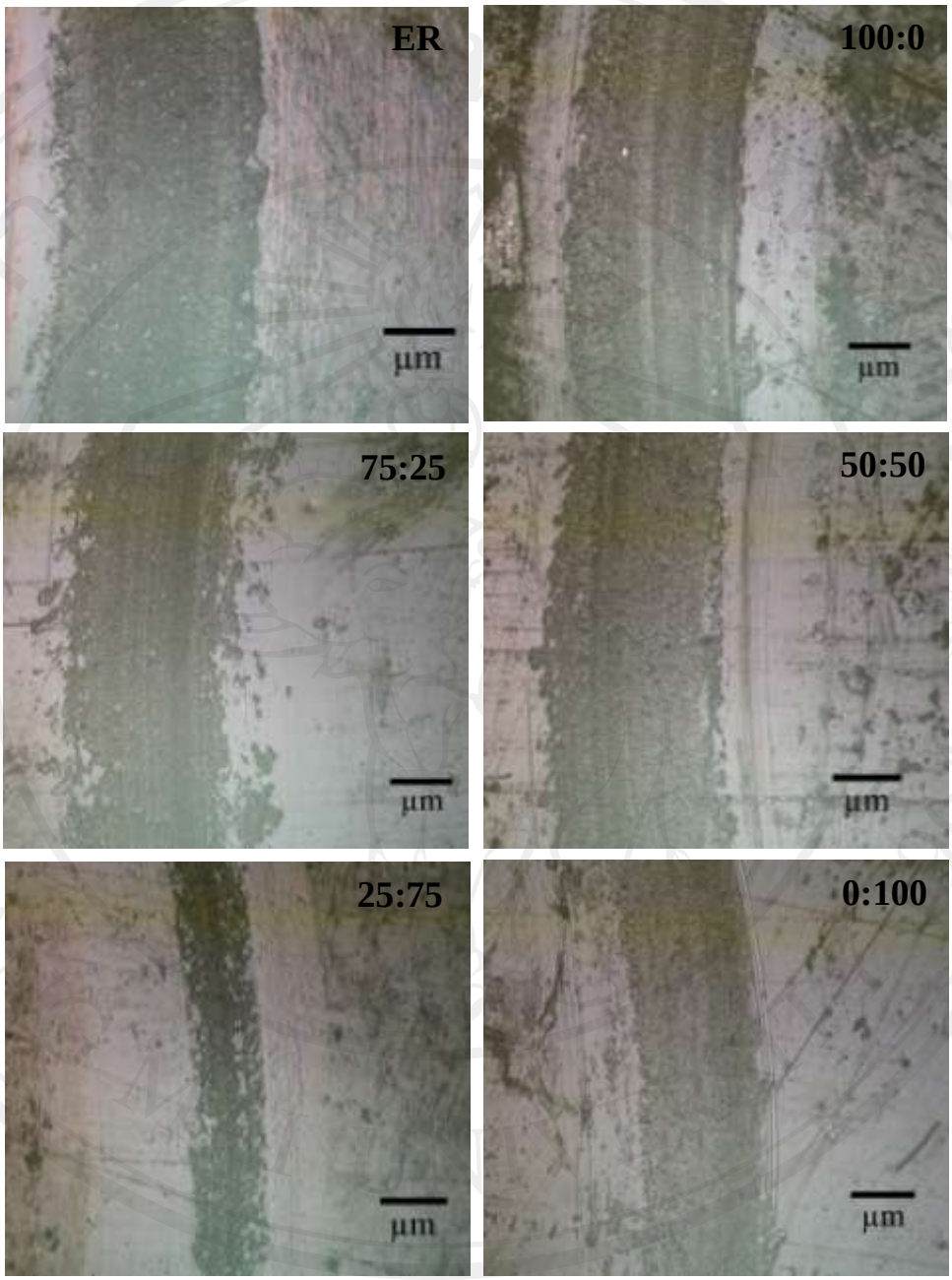

Figure 4.31 The photographs of the wear track width of 0.05 vol% of the fillers (CNTs:SiCNWs ratio) in nanocomposites samples

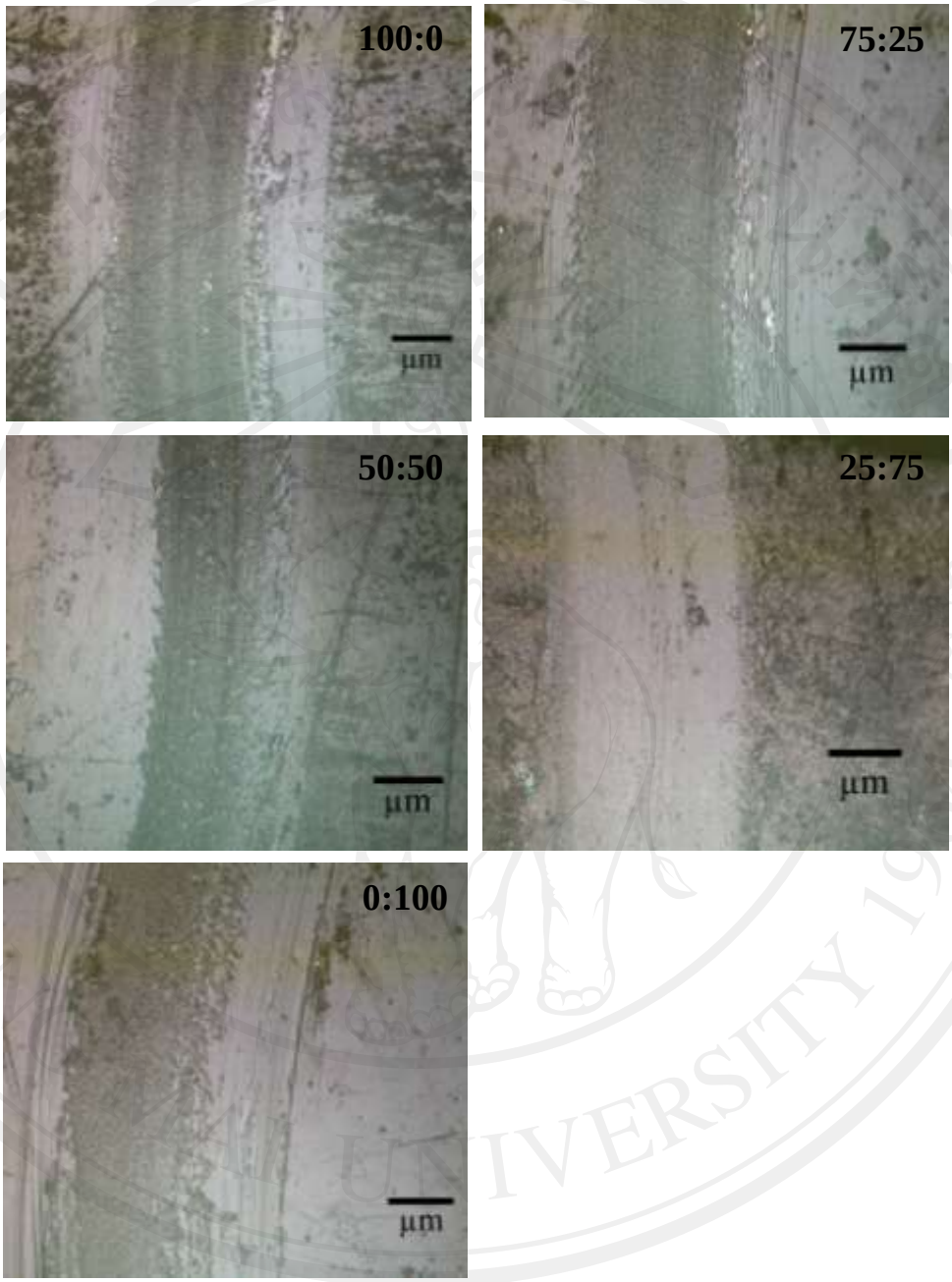

Figure 4.32 The photographs of the wear track width of 0.1 vol% of the fillers (CNTs:SiCNWs ratio) in nanocomposites samples

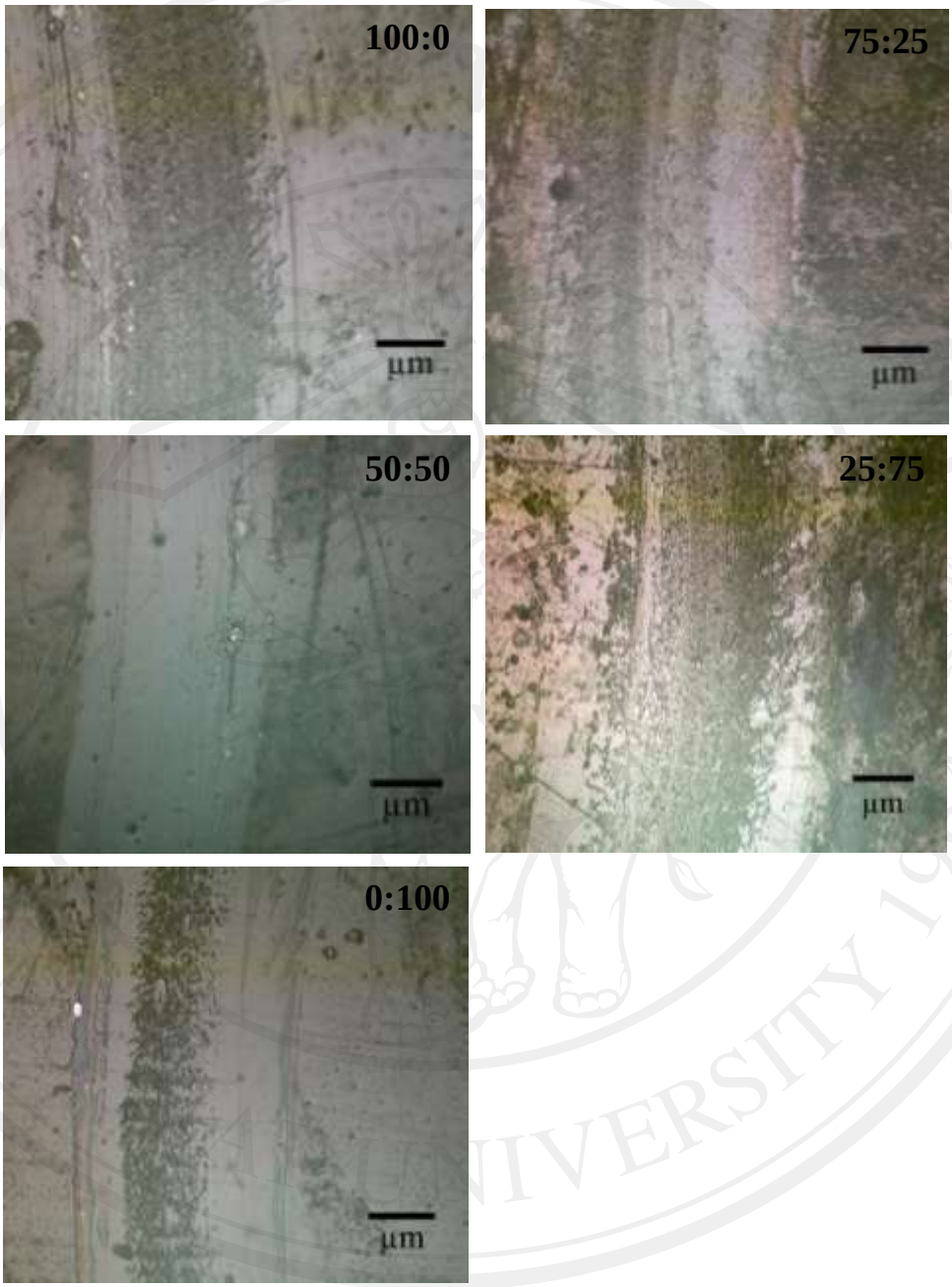

Figure 4.33 The photographs of the wear track width of 0.2 vol% of the fillers (CNTs:SiCNWs ratio) in nanocomposites samples

Udomsupman [103] fabricated the SiCNWs and epoxy resin composites with different ratios of 0.1 -15 vol%, these results shew that significantly increasing of strength corresponds to increasing of SiCNWs contents. The highest gain strength is

70.51 % by 15 vol%, however, increasing of the strength sligthly constant over 0.9 vol% (gain strength 58.55 %) SiCNWs content. Chisholm et al. [3] mixed the nanosized SiC fillers in an epoxy matrix by varying from 1.5-3.0 wt% of the resin. It has been observed that 1.5 wt% nanoparticle loading can promote mechanical properties an average of 20-30%. Therefore, the optimum of adding the filler should not more than 1 vol%. Allaoui et al. [104] investigated mechanical properties of MWNT/epoxy resin with different weigth percentage of MWNT (1-4 wt%). The gain strength shows 80% of 1 wt% MWNT loading. J.B. Bai et al. [105] shows the highest gain strength is 30% of 0.5 wt%. From these results, the optimum content of the nano-fillers should be 1-1.5 wt%, otherwise the nanofillers become the defects in the matrix and could not improve the mechanical properties.

4.2.4 Morphologies of the nanocomposites interface and dispersion of nano-fillers in epoxy matrix

In order to have a better view of effect of CNTs and SiCNWs on the nanocomposites, SEM micrographs were taken and investigated for the nanophased systems. The samples were observed that the CNTs were not very well dispersed in the matrix. There are agglomerations of CNTs in some areas of matrix is shown in fig. 4.30a. Besides, the SEM image (inset) shows particles-to-particles interaction which became almost like impurities. Increase of mechanical properties in this case are hence less than adding SiCNWs. From fig.4.30b, the SEM image exhibits well dispersion of SiCNWs in the matrix and shows particles-polymer-particles interaction. However, the EDS analysis shows the elements of nanocomposites sample (fig. 4.30c), it is found that there are dispersion of all CNTs and SiCNWs in the matrix and

can promote the mechanical properties of epoxy resin especially, tensile and compression strength.

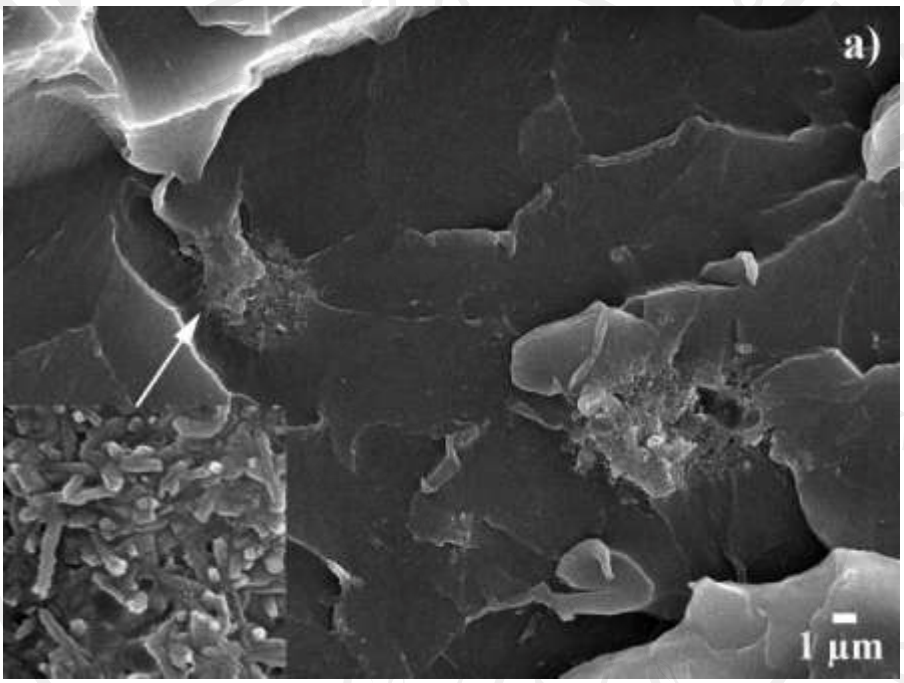

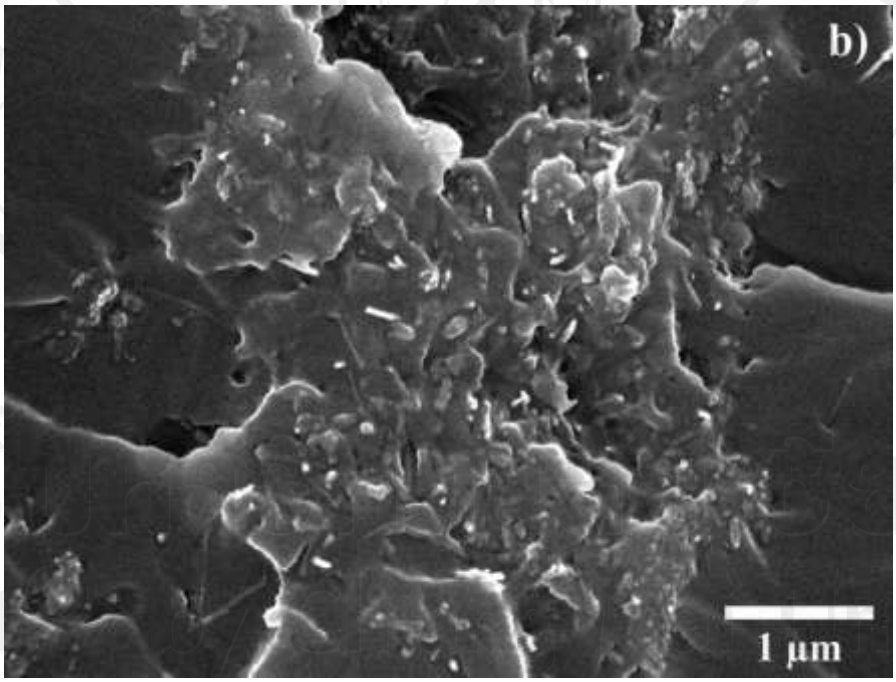

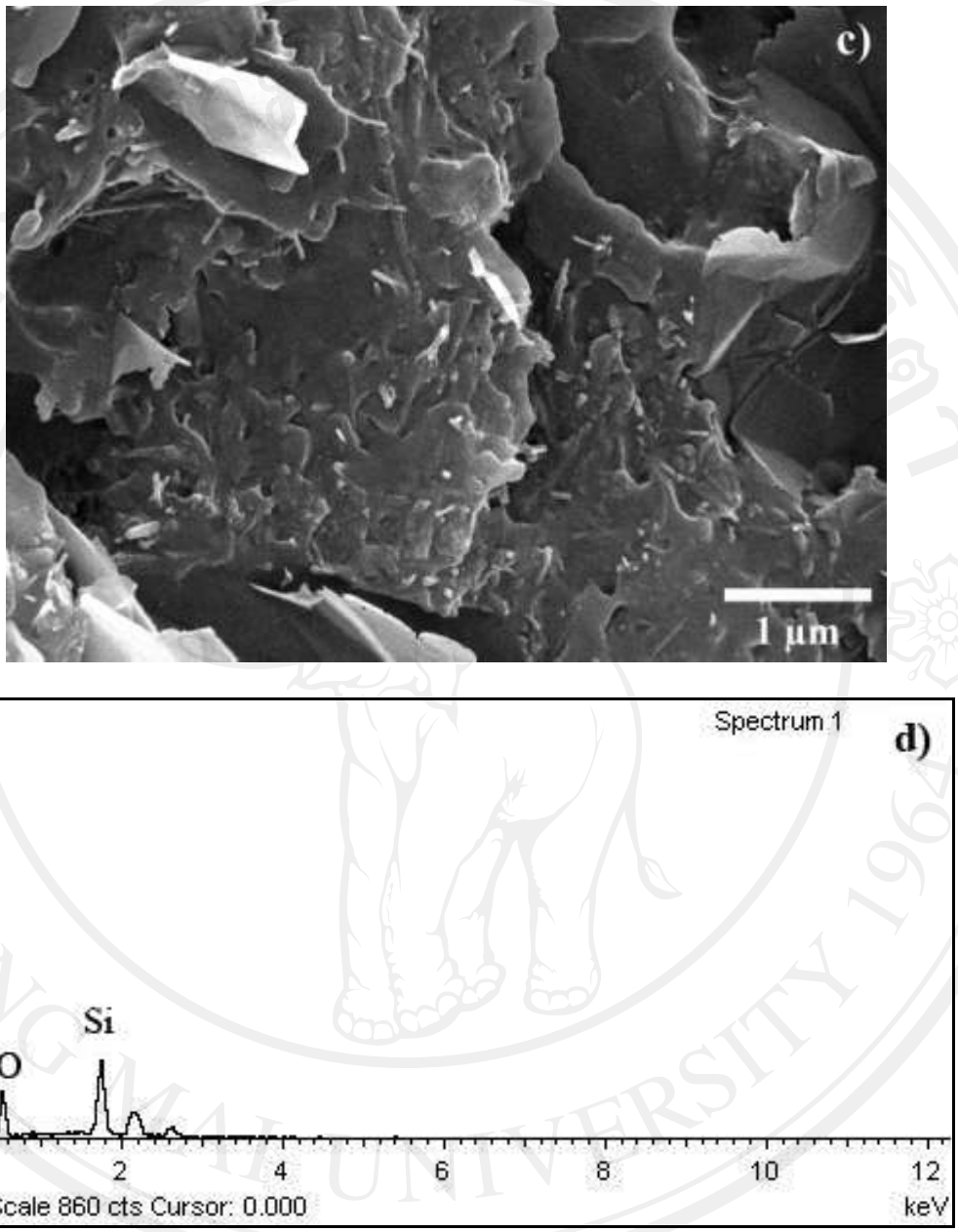

Figure 4.34 The SEM images of the surfaces of CNTs, SiCNWs and epoxy resin nanocomposites containing 0.2 vol% of the nano-fillers: a) CNTs 100% b) SiCNWs 100% c) CNTs:SiCNWs is 25:75 and d) EDS spectrum of the 25:75 ratio (CNTs:SiCNWs)